Available online at www.sciencedirect.com

SCIENCE DIRECT®

ELSEVIER

Mechanical Systems and Signal Processing 18 (2004) 457–489

Mechanical Systems and Signal Processing

www.elsevier.com/locate/jnlabr/ymssp

Non-linear parameter estimation in multi-degree-of-freedom systems using multi-input Volterra series

Animesh Chatterjee[a,*], Nalinaksh S. Vyas[b]

[a] Department of Mechanical Engineering, Visvesvaraya National Institute of Technology, Nagpur 440011, India
[b] Department of Mechanical Engineering, Indian Institute of Technology, Kanpur 208016, India

Received 23 April 2002; received in revised form 5 February 2003; accepted 18 February 2003

Abstract

Functional form input–output representation through Volterra series has been widely used for non-linear system analysis and non-parametric system identification. Recent research work shows that the series representation can be suitably employed for parametric identification also. However, the classical Volterra series is based on a single-input and its application is limited to analysis and identification of single-degree-of-freedom system only. The concept of single-input Volterra series has been extended to multi-input Volterra series by Worden et al. through definition of direct and cross-kernels. The present study employs the multi-input Volterra series and develops a structured response representation of various harmonics under multi-input harmonic excitations. Kernel synthesis formulations are developed for a polynomial form non-linearity with general square and cubic terms. It is shown that higher-order direct and cross-kernel transforms are functions of the first-order kernel transforms and the non-linear parameter vectors. A parameter estimation procedure based on recursive iteration is suggested and illustrated for a two-degree-of-freedom system with square and cubic stiffness non-linearity. Numerical simulations and error analysis are presented for typical rotor-bearing system parameters.

1. Introduction

The functional form representation of input–output relationship through Volterra series provides a structured mathematical platform for non-linear system identification. The series represents non-linear response through a set of multidimensional kernels, known as Volterra kernels. Fourier transforms of these kernels provide the definition of higher-order kernel transforms or higher-order frequency response functions (FRFs) [1]. Earlier works using Volterra

*Corresponding author. Tel.: +91-512-597-040; fax: +91-512-590-007.
E-mail addresses: animeshch@rediffmail.com (A. Chatterjee), vyas@iitk.ac.in (N.S. Vyas).

doi:10.1016/S0888-3270(03)00016-5

series mainly concentrated on non-parametric mapping through identification of the Volterra kernels in time domain [2,3], or the kernel transforms in frequency domain [4–8]. These procedures either approximate the response series to its first term, or extract the first few response components through response component separation method. The consequent error in identification due to finite term approximation depends on the convergence characteristics of the response series. Volterra series, being a power series, suffers from the inherent problem of limited convergence. Tomlinson et al. [9] studied the convergence of first-order FRF of a Duffing oscillator under harmonic excitation and presented a simple formula for determining the upper limit of excitation level for series convergence at natural frequency of the system. Chatterjee and Vyas [10] defined a critical value of the non-dimensional non-linear parameter for response harmonic series convergence and observed that the limiting value of the parameter is a function of excitation frequency and number of terms, k, in the response series approximation.

It can be shown that for polynomial form of non-linearity, higher-order kernel transforms or FRFs are related to the first-order FRF through the non-linear parameters. The procedures for identification of kernel transforms, thus, can be easily extended to estimate the non-linear parameters from the extracted first- and higher-order kernel transforms. Gifford and Tomlinson [11] used stochastic excitation and curve fitted a non-linear multi-degree-of-freedom parametric model to measure the FRF data. Lee [12] used method of harmonic probing and extracted the response components of first harmonic through component separation technique. First- and higher-order kernel transforms were then computed from the separated response components and non-linear parameters were estimated using the relationship between the higher- and first-order kernel transforms. Chatterjee and Vyas [13] have suggested a recursive iteration technique, which computes the first- and higher-order kernel transforms recursively from the measured response harmonic amplitudes. The response series is considered with an optimum number of terms governed by the convergence criterion.

The concept of single-input Volterra series has been recently extended to multi-input Volterra series by Worden et al. [14]. It has been shown that the extended response series involves direct kernels as well as cross-kernels. The present study employs the multi-input Volterra series and develops the response structure under harmonic excitations. Generic expressions for response harmonic amplitudes are presented and kernel synthesis formulations are developed. It is shown that higher-order direct and cross-kernel transforms are functions of the first-order kernel transforms and the set of non-linear parameters representing polynomial non-linearity. The parameter estimation procedure based on recursive iteration, developed for a single-degree-of-freedom system, is extended and illustrated here for a two-degree-of-freedom system with square and cubic stiffness non-linearity. Numerical simulations and error analysis are presented for typical rotor-bearing system parameters.

2. Single-input Volterra series response representation

Volterra series response for a general physical system with $f(t)$ as input excitation and $x(t)$ as output response is represented by

$$x(t) = x_1(t) + x_2(t) + x_3(t) + \cdots + x_n(t) + \cdots \tag{1}$$

with

$$x_n(t) = \int_{-\infty}^{\infty} \cdots \int_{-\infty}^{\infty} h_n(\tau_1, \ldots, \tau_n) f(t-\tau_1) \ldots f(t-\tau_n)\, d\tau_1 \ldots d\tau_n. \tag{2}$$

$h_n(\tau_1, \ldots, \tau_n)$ is the nth-order Volterra kernel and its Fourier transform provides the nth-order FRFs or Volterra kernel transforms as

$$H_n(\omega_1, \ldots, \omega_n) = \int_{-\infty}^{\infty} \cdots \int_{-\infty}^{\infty} h_n(\tau_1, \ldots, \tau_n) \prod_{i=1}^{n} e^{-j\omega_i \tau_i}\, d\tau_1 \ldots d\tau_n. \tag{3}$$

For a single-tone harmonic excitation

$$f(t) = A \cos \omega t = \frac{A}{2} e^{j\omega t} + \frac{A}{2} e^{-j\omega t} \tag{4}$$

the expression for the nth-order response component, following Eq. (2), can be obtained as

$$x_n(t) = \left(\frac{A}{2}\right)^n \sum_{p+q=n} {}^nC_q H_n^{p,q}(\omega) e^{j\omega_{p,q} t} \tag{5}$$

where the following brief notations have been used:

$$H_n^{p,q}(\omega) = H_n(\underbrace{\omega, \ldots, \omega}_{p \text{ times}}, \underbrace{-\omega, \ldots, -\omega}_{q \text{ times}}), \quad \omega_{p,q} = (p-q)\omega.$$

The total response of the system then becomes

$$x(t) = \sum_{n=1}^{\infty} \left(\frac{A}{2}\right)^n \sum_{p+q=n} {}^nC_q H_n^{p,q}(\omega) e^{j\omega_{p,q} t}. \tag{6}$$

Combinations of different p and q result in various response harmonics at frequencies $\omega_{p,q} = \omega, 2\omega, 3\omega$, etc. and the response series given in Eq. (6) can be written in terms of its harmonics as

$$x(t) = X_0 + |X(\omega)|\cos(\omega t + \phi_1) + |X(2\omega)|\cos(2\omega t + \phi_2) + |X(3\omega)|\cos(3\omega t + \phi_3) + \cdots \tag{7}$$

where the response harmonic amplitudes, $X(n\omega)$, are obtained by collecting all the terms associated with the exponential $e^{j\omega_{p,q} t}$ in Eq. (6) for $\omega_{p,q} = (p-q)\omega = n\omega$ and are given by

$$X_0 = \sum_{n=1}^{\infty} \left(\frac{A}{2}\right)^{2n} {}^{2n}C_n H_{2n}^{n,n}(\omega)$$

$$X(n\omega) = \sum_{i=1}^{\infty} \sigma_i(n\omega) \quad \text{and} \quad \phi_n = \angle X(n\omega) \tag{8}$$

with

$$\sigma_i(n\omega) = 2\left(\frac{A}{2}\right)^{n+2i-2} {}^{n+2i-2}C_{i-1} H_{n+2i-2}^{n+i-1,i-1}(\omega). \tag{9}$$

For a system with polynomial form of non-linearity given by

$$m\ddot{x}(t) + c\dot{x}(t) + k_1 x(t) + k_2 x^2(t) + k_3 x^3(t) = f(t) \tag{10}$$

the higher-order kernel transforms are related to the lower-order kernel transforms through non-linear parameters [10] as follows:

$$H_n^{p,q}(\omega) = -\frac{H_1(\omega_{p,q})}{{}^nC_q}\left[k_2 \sum_{\substack{p_i+q_i=n_i \\ n_1+n_2=n}} \{{}^{n_1}C_{q_1} H_{n_1}^{p_1,q_1}(\omega)\}\{{}^{n_2}C_{q_2} H_{n_2}^{p_2,q_2}(\omega)\}\right.$$

$$\left. + k_3 \sum_{\substack{p_i+q_i=n_i \\ n_1+n_2+n_3=n}} \{{}^{n_1}C_{q_1} H_{n_1}^{p_1,q_1}(\omega)\}\{{}^{n_2}C_{q_2} H_{n_2}^{p_2,q_2}(\omega)\}\{{}^{n_3}C_{q_3} H_{n_3}^{p_3,q_3}(\omega)\}\right] \quad \text{for } n > 1. \quad (11)$$

A higher-order kernel transform thus can be synthesised using Eq. (11), from the values of first-order transforms and the non-linear parameters.

3. Multi-input Volterra series response representation

The response measured at the jth station in a multi-degree-of-freedom system under inputs $f_a(t), f_b(t), \ldots$, applied at stations $a, b, \ldots$, can be written as [14]

$$x^{(j)}(t) = x_1^{(j)}(t) + x_2^{(j)}(t) + x_3^{(j)}(t) + \cdots \quad (12)$$

where $x_n^{(j)}(t)$ is the nth-order response component at the jth station. First-order response component at the jth station is formed as a summation of responses due to all the first-order components resulting from each individual input force and is expressed as

$$x_1^{(j)}(t) = x_1^{(j:a)}(t) + x_1^{(j:b)}(t) + \cdots \quad (13)$$

with

$$x_1^{(j:a)}(t) = \int_{-\infty}^{\infty} h_1^{(j:a)}(\tau_1) f_a(t-\tau_1)\,\mathrm{d}\tau_1$$

$$x_1^{(j:b)}(t) = \int_{-\infty}^{\infty} h_1^{(j:b)}(\tau_1) f_b(t-\tau_1)\,\mathrm{d}\tau_1, \text{ etc.}$$

The first-order component can, therefore, be written as

$$x_1^{(j)}(t) = \sum_{\eta=a,b,\ldots} \int_{-\infty}^{\infty} h_1^{(j:\eta)}(\tau_1) f_\eta(t-\tau_1)\,\mathrm{d}\tau_1. \quad (14)$$

The kernels $h_1^{(j:\eta)}(\tau_1)$ for $\eta = a, b, \ldots$, represent the linear impulse response functions, and the corresponding kernel transforms are

$$H_1^{(j:\eta)}(\omega_1) = \int_{-\infty}^{\infty} h_1^{(j:\eta)}(\tau_1) \mathrm{e}^{-j\omega_1\tau_1}\,\mathrm{d}\tau_1. \quad (15)$$

The second-order response component $x_2^{(j)}(t)$ is given by

$$x_2^{(j)}(t) = \sum_{\eta_1=a,b,\ldots} \sum_{\eta_2=a,b,\ldots} \int_{-\infty}^{\infty}\int_{-\infty}^{\infty} h_2^{(j:\eta_1\eta_2)}(\tau_1,\tau_2) f_{\eta_1}(t-\tau_1) f_{\eta_2}(t-\tau_2)\,\mathrm{d}\tau_1\,\mathrm{d}\tau_2. \quad (16)$$

Kernels $h_2^{(j:\eta_1\eta_2)}(\tau_1,\tau_2)$, for $\eta_1=\eta_2$, are called second-order direct kernels, whereas for $\eta_1\neq\eta_2$, they are called second-order cross-kernels. Fourier transforms of these direct and cross-kernels give the respective direct and cross-kernel transforms as

$$H_2^{(j:\eta_1\eta_2)}(\omega_1,\omega_2)=\int_{-\infty}^{\infty}\int_{-\infty}^{\infty}h_2^{(j:\eta_1\eta_2)}(\tau_1,\tau_2)\mathrm{e}^{-j(\omega_1\tau_1+\omega_2\tau_2)}\,\mathrm{d}\tau_1\,\mathrm{d}\tau_2\quad\text{for }\eta_1,\eta_2=a,b,\ldots.\tag{17}$$

Proceeding similarly, the general nth-order response component can be written as

$$x_n^{(j)}(t)=\sum_{\eta_1=a,b,\ldots}\sum_{\eta_2=a,b,\ldots}\cdots\sum_{\eta_n=a,b,\ldots}\int_{-\infty}^{\infty}\int_{-\infty}^{\infty}\cdots\int_{-\infty}^{\infty}h_n^{(j:\eta_1\eta_2\ldots\eta_n)}(\tau_1,\ldots,\tau_n)\times f_{\eta_1}(t-\tau_1)\ldots f_{\eta_n}(t-\tau_n)\,\mathrm{d}\tau_1\ldots\mathrm{d}\tau_n.\tag{18}$$

where the kernels $h_n^{(j:\eta_1\ldots\eta_n)}(\tau_1,\ldots,\tau_n)$ represent the nth-order direct and cross-kernel functions. The nth-order kernel transforms are

$$H_n^{(j:\eta_1\ldots\eta)}(\omega_1,\ldots,\omega_n)=\int_{-\infty}^{\infty}\cdots\int_{-\infty}^{\infty}h_n^{(j:\eta_1\ldots\eta_n)}(\tau_1,\ldots,\tau_n)\mathrm{e}^{-j(\omega_1\tau_1+\cdots+\omega_n\tau_n)}\,\mathrm{d}\tau_1\ldots\mathrm{d}\tau_n.\tag{19}$$

For m number of inputs, there would be m^n number of nth-order kernels for each measurement location j and a system with N degrees of freedom would be characterised by a set of Nm^n number of nth-order kernels. This shows that analysis of multi-degree-of-freedom systems with multi-input excitation involves a large number of kernels. However, the number of kernels can be significantly reduced using symmetry considerations as

$$h_2^{(j:ab)}(\tau_1,\tau_2)+h_2^{(j:ba)}(\tau_1,\tau_2)\to 2h_2^{(j:ab)}(\tau_1,\tau_2)$$

$$h_3^{(j:aab)}(\tau_1,\tau_2,\tau_3)+h_3^{(j:baa)}(\tau_1,\tau_2,\tau_3)+h_3^{(j:aba)}(\tau_1,\tau_2,\tau_3)\to 3h_3^{(j:aab)}(\tau_1,\tau_2,\tau_3)$$

and so on. The rule of symmetry is also applied to the kernel transforms and all kernel transforms with the same set of frequency arguments are considered identical irrespective of the order of arrangement of the arguments.

4. Response structure under harmonic excitation

A multi-degree-of-freedom system with two inputs $f_a(t)$ and $f_b(t)$ is considered here for general illustration of the response characteristics. For harmonic excitation

$$f_a(t)=A\cos\omega_1 t,\quad f_b(t)=B\cos\omega_2 t$$

the response components at a station, j, are obtained from Eq. (18) as

$$x_1^{(j)}(t)=\frac{A}{2}H_1^{(j:a)}(\omega_1)\mathrm{e}^{j\omega_1 t}+\frac{B}{2}H_1^{(j:b)}(\omega_2)\mathrm{e}^{j\omega_2 t}+\text{complex conjugates}\tag{20a}$$

$$
\begin{aligned}
x_2^{(j)}(t) = & \frac{A^2}{2} H_2^{(j:aa)}(\omega_1, -\omega_1) + \frac{B^2}{2} H_2^{(j:bb)}(\omega_2, -\omega_2) \\
& + \frac{A^2}{4} H_2^{(j:aa)}(\omega_1, \omega_1) e^{j2\omega_1 t} + \frac{B^2}{4} H_2^{(j:bb)}(\omega_2, \omega_2) e^{j2\omega_2 t} \\
& + \frac{AB}{2} H_2^{(j:ab)}(\omega_1, \omega_2) e^{j(\omega_1+\omega_2)t} + \frac{AB}{2} H_2^{(j:ab)}(\omega_1, -\omega_2) e^{j(\omega_1-\omega_2)t} \\
& + \text{complex conjugates}
\end{aligned} \tag{20b}
$$

$$
\begin{aligned}
x_3^{(j)}(t) = & \frac{A^3}{8} H_3^{(j:aaa)}(\omega_1, \omega_1, \omega_1) e^{j3\omega_1 t} + \frac{3A^3}{8} H_3^{(j:aaa)}(\omega_1, \omega_1, -\omega_1) e^{j\omega_1 t} \\
& + \frac{B^3}{8} H_3^{(j:bbb)}(\omega_2, \omega_2, \omega_2) e^{j3\omega_2 t} + \frac{3B^3}{8} H_3^{(j:bbb)}(\omega_2, \omega_2, -\omega_2) e^{j\omega_2 t} \\
& + \frac{3AB^2}{4} H_3^{(j:abb)}(\omega_1, \omega_2, -\omega_2) e^{j\omega_1 t} + \frac{3A^2B}{4} H_3^{(j:aab)}(\omega_1, -\omega_1, \omega_2) e^{j\omega_2 t} \\
& + \frac{3A^2B}{8} H_3^{(j:aab)}(\omega_1, \omega_1, \omega_2) e^{j(2\omega_1+\omega_2)t} + \frac{3A^2B}{8} H_3^{(j:aab)}(\omega_1, \omega_1, -\omega_2) e^{j(2\omega_1-\omega_2)t} \\
& + \frac{3AB^2}{8} H_3^{(j:abb)}(\omega_1, \omega_2, \omega_2) e^{j(2\omega_2+\omega_1)t} + \frac{3AB^2}{8} H_3^{(j:abb)}(-\omega_1, \omega_2, \omega_2) e^{j(2\omega_2-\omega_1)t} \\
& + \text{complex conjugates.}
\end{aligned} \tag{20c}
$$

The generic expression for the nth-order response component can be developed as

$$
x_n^{(j)}(t) = \frac{1}{2^n} \sum A^{p+q} B^{s+u} C_{p,q,s,u} H_n^{(j:a_{(p+q)} b_{(s+u)})p,q,s,u}(\omega) e^{j\omega_{p,q,s,u} t} \tag{21}
$$

where $H_n^{(j:a_{(p+q)} b_{(s+u)})p,q,s,u}(\omega)$ denotes the nth-order kernel transforms with $f_a(t)$ considered $(p+q)$ times and $f_b(t)$ considered $(s+u)$ times in the convolution integral, i.e.

$$
H_n^{(j:a_{(p+q)} b_{(s+u)})p,q,s,u}(\omega) = H_n^{(j:\underbrace{aa\ldots}_{p+q \text{ times}}\underbrace{bbb\ldots}_{s+u \text{ times}})}(\underbrace{\omega_1, \ldots,}_{p \text{ times}} \underbrace{-\omega_1, \ldots,}_{q \text{ times}} \underbrace{\omega_2, \ldots,}_{s \text{ times}} \underbrace{-\omega_2, \ldots,}_{u \text{ times}})
$$

and

$$
\omega_{p,q,s,u} = (p-q)\omega_1 + (s-u)\omega_2, \quad C_{p,q,s,u} = \frac{n!}{p!q!s!u!}.
$$

Total response $x^{(j)}(t)$, at the jth coordinate of measurement, then becomes

$$
x^{(j)}(t) = \sum_{n=1}^{\infty} \frac{1}{2^n} \sum A^{p+q} B^{s+u} C_{p,q,s,u} H_n^{(j:a_{(p+q)} b_{(s+u)})p,q,s,u}(\omega) e^{j\omega_{p,q,s,u} t}. \tag{22}
$$

The response will consist of fundamental harmonics at ω_1, ω_2 along with higher-order harmonics of the general form $(m_1\omega_1 + m_2\omega_2)$. Collecting terms with $p - q = m_1$ and $s - u = m_2$ from series (22), one obtains the response amplitude for a general higher-order combination tone as

$$X^{(j)}(m_1\omega_1 + m_2\omega_2) = \sum_{i=1}^{\infty} \frac{1}{2^{n+2i-3}} \sum_{p+s=i-1} A^{m_1+2p} B^{m_2+2s} C_{m_1+p,p,m_2+s,s} \times H_{n+2i-2}^{(j:a_{(m_1+2p)}b_{(m_2+2s)})m_1+p,p,m_2+s,s}(\omega) \tag{23}$$

where $n = |m_1| + |m_2|$.

5. Higher-order kernel synthesis

Similar to the case in single-degree-of-freedom systems with polynomial non-linearity, higher-order kernels in multi-degree-of-freedom system can also be represented in terms of lower-order kernel transforms and non-linear parameters. This is illustrated here for a two-degree-of-freedom system with general form of polynomial non-linearity up to the cubic term:

$$m_x\ddot{x}(t) + c_{xx}\dot{x}(t) + c_{xy}\dot{y}(t) + k_{xx}x(t) + k_{xy}y(t) + k_{2x}^{(xx)}x^2(t) + k_{2x}^{(xy)}x(t)y(t) + k_{2x}^{(yy)}y^2(t) + k_{3x}^{(xxx)}x^3(t) + k_{3x}^{(xxy)}x^2(t)y(t) + k_{3x}^{(xyy)}x(t)y^2(t) + k_{3x}^{(yyy)}y^3(t) = f_x(t) \tag{24a}$$

$$m_y\ddot{y}(t) + c_{yx}\dot{x}(t) + c_{yy}\dot{y}(t) + k_{yx}x(t) + k_{yy}y(t) + k_{2y}^{(xx)}x^2(t) + k_{2y}^{(xy)}x(t)y(t) + k_{2y}^{(yy)}y^2(t) + k_{3y}^{(xxx)}x^3(t) + k_{3y}^{(xxy)}x^2(t)y(t) + k_{3y}^{(xyy)}x(t)y^2(t) + k_{3y}^{(yyy)}y^3(t) = f_y(t). \tag{24b}$$

The parameters involved in the above equations are:

Linear parameters:

$$[M] = \begin{bmatrix} m_x & 0 \\ 0 & m_y \end{bmatrix}, \quad [C] = \begin{bmatrix} c_{xx} & c_{xy} \\ c_{yx} & c_{yy} \end{bmatrix}, \quad \text{and} \quad [K] = \begin{bmatrix} k_{xx} & k_{xy} \\ k_{yx} & k_{yy} \end{bmatrix}. \tag{25}$$

Non-linear parameters of second order:

The set of second-order non-linear parameters can be arranged in a vector form as

$$\{K_2\} = \begin{Bmatrix} \{K_{2x}\} \\ \{K_{2y}\} \end{Bmatrix}$$

with

$$\{K_{2x}\} = \{k_{2x}^{(xx)}, k_{2x}^{(yy)}, k_{2x}^{(xy)}\}^T \quad \text{and} \quad \{K_{2y}\} = \{k_{2y}^{(xx)}, k_{2y}^{(yy)}, k_{2y}^{(xy)}\}^T. \tag{26}$$

The first number in the subscript indicates the order of the non-linear term and the second number indicates the response coordinate to which it corresponds. The superscript notations indicate the product combination of the response coordinates associated with the parameter.

Non-linear parameters of third order:
The set of third-order non-linear parameters can similarly be arranged in a vector form as

$$\{K_3\} = \left\{ \begin{array}{c} \{K_{3x}\} \\ \{K_{3y}\} \end{array} \right\}$$

with

$$\{K_{3x}\} = \{k_{3x}^{(xxx)}, k_{3x}^{(yyy)}, k_{3x}^{(xxy)}, k_{3x}^{(xyy)}\}^T \quad \text{and} \quad \{K_{3y}\} = \{k_{3y}^{(xxx)}, k_{3y}^{(yyy)}, k_{3y}^{(xxy)}, k_{3y}^{(xyy)}\}^T \tag{27}$$

with similar notations as in the case of second-order non-linear parameters above.

5.1. First-order kernel transforms

For extraction of first-order kernels, harmonic excitation of the form $f_x(t) = A\cos\omega_1 t$ and $f_y(t) = B\cos\omega_2 t$ is considered. The Volterra series response for this multi-point excitation, from Eq. (22), is

$$\begin{aligned} x(t) =& \frac{A}{2} H_1^{(x:x)}(\omega_1)e^{j\omega_1 t} + \frac{B}{2} H_1^{(x:y)}(\omega_2)e^{j\omega_2 t} + \frac{A^2}{2} H_2^{(x:xx)}(\omega_1, -\omega_1) + \frac{B^2}{2} H_2^{(x:yy)}(\omega_2, -\omega_2) \\ &+ \frac{A^2}{4} H_2^{(x:xx)}(\omega_1, \omega_1)e^{j2\omega_1 t} + \frac{B^2}{4} H_2^{(x:yy)}(\omega_2, \omega_2)e^{j2\omega_2 t} + \frac{AB}{2} H_2^{(x:xy)}(\omega_1, \omega_2)e^{j(\omega_1+\omega_2)^t} \\ &+ \frac{AB}{2} H_2^{(x:xy)}(\omega_1, -\omega_2)e^{j(\omega_1-\omega_2)^t} + \frac{A^3}{8} H_3^{(x:xxx)}(\omega_1, \omega_1, \omega_1)e^{j3\omega_1 t} \\ &+ \frac{3A^3}{8} H_3^{(x:xxx)}(\omega_1, \omega_1, -\omega_1)e^{j\omega_1 t} + \frac{B^3}{8} H_3^{(x:yyy)}(\omega_2, \omega_2, \omega_2)e^{j3\omega_2 t} \\ &+ \frac{3B^3}{8} H_3^{(x:yyy)}(\omega_2, \omega_2, -\omega_2)e^{j\omega_2 t} + \frac{3A^2B}{4} H_3^{(x:xxy)}(\omega_1, -\omega_1, \omega_2)e^{j\omega_2 t} \\ &+ \frac{3A^2B}{8} H_3^{(x:xxy)}(\omega_1, \omega_1, \omega_2)e^{j(2\omega_1+\omega_2)t} + \frac{3A^2B}{8} H_3^{(x:xxy)}(\omega_1, \omega_1, -\omega_2)e^{j(2\omega_1-\omega_2)t} \\ &+ \frac{3AB^2}{4} H_3^{(x:xyy)}(\omega_1, \omega_2, -\omega_2)e^{j\omega_1 t} + \frac{3AB^2}{8} H_3^{(x:xyy)}(\omega_1, \omega_2, \omega_2)e^{j(2\omega_2+\omega_1)t} \\ &+ \frac{3AB^2}{8} H_3^{(x:xyy)}(-\omega_1, \omega_2, \omega_2)e^{j(2\omega_2-\omega_1)t} + \text{complex conjugate terms} \\ &+ \text{higher-order terms} \end{aligned} \tag{28a}$$

$$\begin{aligned} y(t) =& \frac{A}{2} H_1^{(y:x)}(\omega_1)e^{j\omega_1 t} + \frac{B}{2} H_1^{(y:y)}(\omega_2)e^{j\omega_2 t} + \frac{A^2}{2} H_2^{(y:xx)}(\omega_1, -\omega_1) + \frac{B^2}{2} H_2^{(y:yy)}(\omega_2, -\omega_2) \\ &+ \frac{A^2}{4} H_2^{(y:xx)}(\omega_1, \omega_1)e^{j2\omega_1 t} + \frac{B^2}{4} H_2^{(y:yy)}(\omega_2, \omega_2)e^{j2\omega_2 t} + \frac{AB}{2} H_2^{(y:xy)}(\omega_1, \omega_2)e^{j(\omega_1+\omega_2)^t} \\ &+ \frac{AB}{2} H_2^{(y:xy)}(\omega_1, -\omega_2)e^{j(\omega_1-\omega_2)^t} + \frac{A^3}{8} H_3^{(y:xxx)}(\omega_1, \omega_1, \omega_1)e^{j3\omega_1 t} \end{aligned}$$

$$+\frac{3A^3}{8}H_3^{(y:xxx)}(\omega_1,\omega_1,-\omega_1)e^{j\omega_1 t}+\frac{B^3}{8}H_3^{(y:yyy)}(\omega_2,\omega_2,\omega_2)e^{j3\omega_2 t}$$
$$+\frac{3B^3}{8}H_3^{(y:yyy)}(\omega_2,\omega_2,-\omega_2)e^{j\omega_2 t}+\frac{3A^2B}{4}H_3^{(y:xxy)}(\omega_1,-\omega_1,\omega_2)e^{j\omega_2 t}$$
$$+\frac{3A^2B}{8}H_3^{(y:xxy)}(\omega_1,\omega_1,\omega_2)e^{j(2\omega_1+\omega_2)t}+\frac{3A^2B}{8}H_3^{(y:xxy)}(\omega_1,\omega_1,-\omega_2)e^{j(2\omega_1-\omega_2)t}$$
$$+\frac{3AB^2}{4}H_3^{(y:xyy)}(\omega_1,\omega_2,-\omega_2)e^{j\omega_1 t}+\frac{3AB^2}{8}H_3^{(y:xyy)}(\omega_1,\omega_2,\omega_2)e^{j(2\omega_2+\omega_1)t}$$
$$+\frac{3AB^2}{8}H_3^{(y:xyy)}(-\omega_1,\omega_2,\omega_2)e^{j(2\omega_2-\omega_1)t}+\text{complex conjugate terms}$$
$$+\text{higher-order terms.} \tag{28b}$$

After substitution of the response expressions (28a) and (28b) in the governing equations of motion (24a) and (24b), the linear parameter matrices can be shown to be related to first-order kernel transforms as

$$[-\omega^2[M]+j\omega[C]+[K]]=\begin{bmatrix} H_1^{(x:x)}(\omega) & H_1^{(x:y)}(\omega) \\ H_1^{(y:x)}(\omega) & H_1^{(y:y)}(\omega)\end{bmatrix}^{-1}. \tag{29}$$

5.2. Synthesis of second-order kernel transforms

It can be seen from the response series (Eq. (28)) that there are three types of second-order kernel transforms for each degree of freedom, $H_2^{(j:xx)}(\omega_1,\omega_2)$, $H_2^{(j:xy)}(\omega_1,\omega_2)$, and $H_2^{(j:yy)}(\omega_1,\omega_2)$, $j=x,y$. While $H_2^{(j:xx)}(\omega_1,\omega_2)$ and $H_2^{(j:yy)}(\omega_1,\omega_2)$ are the direct kernel transforms, $H_2^{(j:xy)}(\omega_1,\omega_2)$ is the cross-kernel transform. Equating coefficients of the corresponding second-order harmonic in governing equations of motion (24a) and (24b), after substitution of response expressions (Eqs. (28a) and (28b)), the second-order kernel transforms can be obtained in terms of first-order kernel transforms in the following form:

$$\begin{Bmatrix} H_2^{(x:\eta_1\eta_2)}(\omega_1,\omega_2) \\ H_2^{(y:\eta_1\eta_2)}(\omega_1,\omega_2)\end{Bmatrix}=\begin{bmatrix} H_1^{(x:x)}(\omega_1+\omega_2) & H_1^{(x:y)}(\omega_1+\omega_2) \\ H_1^{(y:x)}(\omega_1+\omega_2) & H_1^{(y:y)}(\omega_1+\omega_2)\end{bmatrix}\begin{Bmatrix} p_{\eta_1\eta_2} \\ q_{\eta_1\eta_2}\end{Bmatrix},\quad \eta_1,\eta_2=x,y \tag{30}$$

with

$$p_{\eta_1\eta_2}=-k_{2x}^{(xx)}H_1^{(x:\eta_1)}(\omega_1)H_1^{(x:\eta_2)}(\omega_2)-k_{2x}^{(yy)}H_1^{(y:\eta_1)}(\omega_1)H_1^{(y:\eta_2)}(\omega_2)$$
$$-\frac{k_{2x}^{(xy)}}{2}\{H_1^{(x:\eta_1)}(\omega_1)H_1^{(y:\eta_2)}(\omega_2)+H_1^{(x:\eta_2)}(\omega_1)H_1^{(y:\eta_1)}(\omega_2)\} \tag{31a}$$

and

$$q_{\eta_1\eta_2}=-k_{2y}^{(xx)}H_1^{(x:\eta_1)}(\omega_1)H_1^{(x:\eta_2)}(\omega_2)-k_{2y}^{(yy)}H_1^{(y:\eta_1)}(\omega_1)H_1^{(y:\eta_2)}(\omega_2)$$
$$-\frac{k_{2y}^{(xy)}}{2}\{H_1^{(x:\eta_1)}(\omega_1)H_1^{(y:\eta_2)}(\omega_2)+H_1^{(x:\eta_2)}(\omega_1)H_1^{(y:\eta_1)}(\omega_2)\}. \tag{31b}$$

Eq. (30) can be re-written to express second-order kernel transforms as a function of the non-linear parameter vector, $\{\{K_{2x}\}\ \{K_{2y}\}\}^T$, as

$$\left\{\begin{array}{c} H_2^{(x:\eta_1\eta_2)}(\omega_1,\omega_2) \\ H_2^{(y:\eta_1\eta_2)}(\omega_1,\omega_2) \end{array}\right\} = \begin{bmatrix} H_1^{(x:x)}(\omega_1+\omega_2) & H_1^{(x:y)}(\omega_1+\omega_2) \\ H_1^{(y:x)}(\omega_1+\omega_2) & H_1^{(y:y)}(\omega_1+\omega_2) \end{bmatrix} \begin{bmatrix} \{G\} & \{0\} \\ \{0\} & \{G\} \end{bmatrix} \left\{\begin{array}{c} \{K_{2x}\} \\ \{K_{2y}\} \end{array}\right\} \tag{32}$$

where $\{0\}$ is a null row vector of dimension 1×3 and

$$\{G\} = \{\ G_1^{(\eta_1\eta_2)}\quad G_2^{(\eta_1\eta_2)}\quad G_3^{(\eta_1\eta_2)}\ \} \tag{33}$$

with

$$\begin{aligned} G_1^{(\eta_1\eta_2)} &= -H_1^{(x:\eta_1)}(\omega_1)H_1^{(x:\eta_2)}(\omega_2) \\ G_2^{(\eta_1\eta_2)} &= -H_1^{(y:\eta_1)}(\omega_1)H_1^{(y:\eta_2)}(\omega_2) \\ G_3^{(\eta_1\eta_2)} &= -0.5\{H_1^{(x:\eta_1)}(\omega_1)H_1^{(y:\eta_2)}(\omega_2) + H_1^{(x:\eta_2)}(\omega_1)H_1^{(y:\eta_1)}(\omega_2)\}. \end{aligned}$$

Eqs. (32) relate the general second-order kernel transforms $H_2^{(x:\eta_1\eta_2)}(\omega_1,\omega_2)$ and $H_2^{(y:\eta_1\eta_2)}(\omega_1,\omega_2)$ to the second-order non-linear parameter vector $\{K_2\}$ through a coefficient matrix whose elements are functions of the first-order kernel transforms alone.

5.3. Synthesis of third-order kernel transforms

There are four types of third-order kernel transforms for each degree of freedom: $H_3^{(j:xxx)}(\omega_1,\omega_2,\omega_3)$, $H_3^{(j:yyy)}(\omega_1,\omega_2,\omega_3)$, $H_3^{(j:xxy)}(\omega_1,\omega_2,\omega_3)$ and $H_3^{(j:xyy)}(\omega_1,\omega_2,\omega_3)$; $j = x, y$ (refer Eqs. (28a) and (28b)). While the first two are direct kernel transforms, the other two are cross-kernel transforms. Following the harmonic probing procedure, third-order kernel transforms can be synthesised as

$$\left\{\begin{array}{c} H_3^{(x:\eta_1\eta_2\eta_3)}(\omega_1,\omega_2,\omega_3) \\ H_3^{(y:\eta_1\eta_2\eta_3)}(\omega_1,\omega_2,\omega_3) \end{array}\right\} = \begin{bmatrix} H_1^{(x:x)}(\omega_1+\omega_2+\omega_3) & H_1^{(x:y)}(\omega_1+\omega_2+\omega_3) \\ H_1^{(y:x)}(\omega_1+\omega_2+\omega_3) & H_1^{(y:y)}(\omega_1+\omega_2+\omega_3) \end{bmatrix} \left\{\begin{array}{c} p_{\eta_1\eta_2\eta_3} \\ q_{\eta_1\eta_2\eta_3} \end{array}\right\}$$
$$\eta_i = x, y;\quad i = 1,2,3 \tag{34}$$

where

$$\begin{aligned} p_{\eta_1\eta_2\eta_3} = &-\frac{2k_{2x}^{(xx)}}{3}\sum_{\substack{i,j,k=1,2,3\\ i\neq j\neq k}} H_1^{(x:\eta_i)}(\omega_i)H_2^{(x:\eta_j\eta_k)}(\omega_j,\omega_k) \\ &-\frac{2k_{2x}^{(yy)}}{3}\sum_{\substack{i,j,k=1,2,3\\ i\neq j\neq k}} H_1^{(y:\eta_i)}(\omega_i)H_2^{(y:\eta_j\eta_k)}(\omega_j,\omega_k) \end{aligned}$$

$$
\begin{aligned}
&- \frac{k_{2x}^{(xy)}}{3} \sum_{\substack{m,n=x,y \\ m \neq n}} \sum_{\substack{i,j,k=1,2,3 \\ i \neq j \neq k}} H_1^{(m:\eta_i)}(\omega_i) H_2^{(n:\eta_j\eta_k)}(\omega_j, \omega_k) \\
&- k_{3x}^{(xxx)} H_1^{(x:\eta_1)}(\omega_1) H_1^{(x:\eta_2)}(\omega_2) H_1^{(x:\eta_3)}(\omega_3) \\
&- k_{3x}^{(yyy)} H_1^{(y:\eta_1)}(\omega_1) H_1^{(y:\eta_2)}(\omega_2) H_1^{(y:\eta_3)}(\omega_3) \\
&- k_{3x}^{(xxy)} \sum_{\substack{i,j,k=1,2,3 \\ i \neq j \neq k}} H_1^{(x:\eta_i)}(\omega_i) H_1^{(x:\eta_j)}(\omega_j) H_1^{(y:\eta_k)}(\omega_k) \\
&- k_{3x}^{(xyy)} \sum_{\substack{i,j,k=1,2,3 \\ i \neq j \neq k}} H_1^{(x:\eta_i)}(\omega_i) H_1^{(y:\eta_j)}(\omega_j) H_1^{(y:\eta_k)}(\omega_k)
\end{aligned} \tag{35a}
$$

and

$$
\begin{aligned}
q_{\eta_1\eta_2\eta_3} = &- \frac{2k_{2y}^{(xx)}}{3} \sum_{\substack{i,j,k=1,2,3 \\ i \neq j \neq k}} H_1^{(x:\eta_i)}(\omega_i) H_2^{(x:\eta_j\eta_k)}(\omega_j, \omega_k) \\
&- \frac{2k_{2y}^{(yy)}}{3} \sum_{\substack{i,j,k=1,2,3 \\ i \neq j \neq k}} H_1^{(y:\eta_i)}(\omega_i) H_2^{(y:\eta_j\eta_k)}(\omega_j, \omega_k) \\
&- \frac{k_{2y}^{(yx)}}{3} \sum_{\substack{m,n=x,y \\ m \neq n}} \sum_{\substack{i,j,k=1,2,3 \\ i \neq j \neq k}} H_1^{(m:\eta_i)}(\omega_i) H_2^{(n:\eta_j\eta_k)}(\omega_j, \omega_k) \\
&- k_{3y}^{(xxx)} H_1^{(x:\eta_1)}(\omega_1) H_1^{(x:\eta_2)}(\omega_2) H_1^{(x:\eta_3)}(\omega_3) \\
&- k_{3y}^{(yyy)} H_1^{(y:\eta_1)}(\omega_1) H_1^{(y:\eta_2)}(\omega_2) H_1^{(y2:\eta_3)}(\omega_3) \\
&- k_{3y}^{(xxy)} \sum_{\substack{i,j,k=1,2,3 \\ i \neq j \neq k}} H_1^{(x:\eta_i)}(\omega_i) H_1^{(x:\eta_j)}(\omega_j) H_1^{(y:\eta_k)}(\omega_k) \\
&- k_{3y}^{(xyy)} \sum_{\substack{i,j,k=1,2,3 \\ i \neq j \neq k}} H_1^{(x:\eta_i)}(\omega_i) H_1^{(y:\eta_j)}(\omega_j) H_1^{(y:\eta_k)}(\omega_k).
\end{aligned} \tag{35b}
$$

Relationship between third-order kernel transforms and non-linear parameters can be developed by denoting

$$\{T\} = \{\ T_1^{(\eta_1\eta_2\eta_3)} \quad T_2^{(\eta_1\eta_2\eta_3)} \quad T_3^{(\eta_1\eta_2\eta_3)}\ \} \tag{36}$$

with

$$T_1^{(\eta_1\eta_2\eta_3)} = -\frac{2}{3}\sum_{\substack{i,j,k=1\\ i\neq j\neq k}} H_1^{(x:\eta_i)}(\omega_i)H_2^{(x:\eta_j\eta_k)}(\omega_j,\omega_k)$$

$$T_2^{(\eta_1\eta_2\eta_3)} = -\frac{2}{3}\sum_{\substack{i,j,k=1\\ i\neq j}} H_1^{(y:\eta_i)}(\omega_i)H_2^{(y:\eta_j\eta_k)}(\omega_j,\omega_k)$$

$$T_3^{(\eta_1\eta_2\eta_3)} = -\frac{1}{3}\sum_{\substack{m,n=x,y\\ m\neq n}}\sum_{\substack{i,j,k=1\\ i\neq j}} H_1^{(m:\eta_i)}(\omega_i)H_2^{(n:\eta_j\eta_k)}(\omega_j,\omega_k)$$

and

$$\{S\} = \{\, S_1^{(\eta_1\eta_2\eta_3)} \quad S_2^{(\eta_1\eta_2\eta_3)} \quad S_3^{(\eta_1\eta_2\eta_3)} \quad S_4^{(\eta_1\eta_2\eta_3)} \,\} \tag{37}$$

with

$$S_1^{(\eta_1\eta_2\eta_3)} = -H_1^{(x:\eta_1)}(\omega_1)H_1^{(x:\eta_2)}(\omega_2)H_1^{(x:\eta_3)}(\omega_3)$$

$$S_2^{(\eta_1\eta_2\eta_3)} = -H_1^{(y:\eta_1)}(\omega_1)H_1^{(y:\eta_2)}(\omega_2)H_1^{(y:\eta_3)}(\omega_3)$$

$$S_3^{(\eta_1\eta_2\eta_3)} = -\sum_{\substack{i,j,k=1,2,3\\ i\neq j\neq k}} H_1^{(x:\eta_1)}(\omega_1)H_1^{(x:\eta_2)}(\omega_2)H_1^{(y:\eta_3)}(\omega_3)$$

$$S_4^{(\eta_1\eta_2\eta_3)} = -\sum_{\substack{i,j,k=1,2,3\\ i\neq j\neq k}} H_1^{(x:\eta_1)}(\omega_1)H_1^{(y:\eta_2)}(\omega_2)H_1^{(y:\eta_3)}(\omega_3)$$

to modify Eq. (34) as

$$\begin{Bmatrix} H_3^{(x:\eta_i\eta_j\eta_k)}(\omega_1,\omega_2,\omega_3) \\ H_3^{(y:\eta_i\eta_j\eta_k)}(\omega_1,\omega_2,\omega_3) \end{Bmatrix} - \begin{bmatrix} H_1^{(x:x)}(\omega_1+\omega_2+\omega_3) & H_1^{(x:y)}(\omega_1+\omega_2+\omega_3) \\ H_1^{(y:x)}(\omega_1+\omega_2+\omega_3) & H_1^{(y:y)}(\omega_1+\omega_2+\omega_3) \end{bmatrix}\begin{bmatrix} \{T\} & 0 \\ 0 & \{T\} \end{bmatrix}\begin{Bmatrix} K_{2x} \\ K_{2y} \end{Bmatrix}$$
$$= \begin{bmatrix} H_1^{(x:x)}(\omega_1+\omega_2+\omega_3) & H_1^{(x:y)}(\omega_1+\omega_2+\omega_3) \\ H_1^{(y:x)}(\omega_1+\omega_2+\omega_3) & H_1^{(y:y)}(\omega_1+\omega_2+\omega_3) \end{bmatrix}\begin{bmatrix} \{S\} & 0 \\ 0 & \{S\} \end{bmatrix}\begin{Bmatrix} K_{3x} \\ K_{3y} \end{Bmatrix}. \tag{38}$$

6. Parameter estimation

A parameter estimation procedure employing the relationships given by Eqs. (32) and (38) is suggested here for the determination of the non-linear parameters. First- and higher-order kernel transforms are obtained from measurements of response harmonics. Non-linear parameters are estimated by regression of these transforms through relationships (32) and (38). The kernel transforms are determined in an iterative manner, to include maximum possible converging terms from the Volterra series, to recursively refine the non-linear estimates.

The Volterra series expression for general response harmonic amplitude given in Eq. (23) can be rewritten for x and y-coordinates as

$$X(m_1\omega_1 + m_2\omega_2) = \sum_{i=1}^{\infty} {}^{x}\sigma_i(m_1\omega_1 + m_2\omega_2) \tag{39}$$

and

$$Y(m_1\omega_1 + m_2\omega_2) = \sum_{i=1}^{\infty} {}^{y}\sigma_i(m_1\omega_1 + m_2\omega_2) \tag{40}$$

with

$${}^{x}\sigma_i(m_1\omega_1 + m_2\omega_2) = \frac{1}{2^{n+2i-3}} \sum_{p+s=i-1} A^{m_1+2p} B^{m_2+2s} C_{m_1+p,p,m_2+s,s} \times H_{n+2i-2}^{(x:x_{(2p+m_1)}y_{(2s+m_2)})m_1+p,p,m_2+s,s}(\omega) \tag{41}$$

and

$${}^{y}\sigma_i(m_1\omega_1 + m_2\omega_2) = \frac{1}{2^{n+2i-3}} \sum_{p+s=i-1} A^{m_1+2p} B^{m_2+2s} C_{m_1+p,p,m_2+s,s} \times H_{n+2i-2}^{(y:x_{(2p+m_1)}y_{(2s+m_2)})m_1+p,p,m_2+s,s}(\omega) \tag{42}$$

where $n = |m_1| + |m_2|$.

6.1. Preliminary estimates of linear parameters

For two input single-tone excitation $f_x(t) = A\cos\omega_1 t$ and $f_y(t) = B\cos\omega_2 t$, response harmonic amplitudes $X(\omega_1)$, $X(\omega_2)$, $Y(\omega_1)$ and $Y(\omega_2)$ can be filtered from measurements $x(t)$, $y(t)$. Truncating the infinite series expressions in Eqs. (39) and (40) up to k-terms, one obtains

$$H_1^{(x:x)}(\omega_1) \approx \frac{1}{A}\left[X(\omega_1) - \sum_{i=2}^{k} {}^{x}\sigma_i(\omega_1)\right] \tag{43a}$$

$$H_1^{(x:y)}(\omega_2) \approx \frac{1}{B}\left[X(\omega_2) - \sum_{i=2}^{k} {}^{x}\sigma_i(\omega_2)\right] \tag{43b}$$

$$H_1^{(y:x)}(\omega_1) \approx \frac{1}{A}\left[Y(\omega_1) - \sum_{i=2}^{k} {}^{y}\sigma_i(\omega_1)\right] \tag{43c}$$

$$H_1^{(y:y)}(\omega_2) \approx \frac{1}{B}\left[Y(\omega_2) - \sum_{i=2}^{k} {}^{y}\sigma_i(\omega_2)\right]. \tag{43d}$$

A preliminary estimation of the first-order kernel transforms $H_1^{(x:x)}(\omega_1)$, $H_1^{(x:y)}(\omega_2)$, $H_1^{(y:x)}(\omega_1)$, and $H_1^{(y:y)}(\omega_2)$ is made by ignoring the contribution from higher-order series terms. Similarly, applying excitation $f_x(t) = A\cos\omega_2 t$ and $f_y(t) = B\cos\omega_1 t$, kernel transforms$H_1^{(x:x)}(\omega_2)$, $H_1^{(x:y)}(\omega_1)$, $H_1^{(y:x)}(\omega_2)$ and $H_1^{(y:y)}(\omega_1)$ can be obtained. Using these values of first-order kernel transforms, for a set of excitation frequencies ω_i, preliminary estimates of the linear parameter matrices $[M]$, $[C]$ and $[K]$ are obtained through curve fitting of Eq. (29).

6.2. Preliminary estimates of second-order non-linear parameters

Eq. (32) provides the synthesis relationship of second-order kernel transforms in terms of the non-linear parameter vector $\{K_2\}$. The relationship is generic for any combination of $\eta_1 = x, y$; $\eta_2 = x, y$. Noting that the vector $\{K_2\}$ consists of six unknown parameters, the relationship can be employed for estimation of these parameters if values of six second-order kernel transforms are available. This can be obtained through measurement of second-order response harmonic amplitudes $X(2\omega_1)$, $X(2\omega_2)$, $X(\omega_1+\omega_2)$, $Y(2\omega_1)$, and $Y(2\omega_2)$ and $Y(\omega_1+\omega_2)$. Truncating the infinite series expressions in Eqs. (39) and (40) up to k terms, the corresponding second-order kernel transforms can be written in the form

$$H_2^{(x:xx)}(\omega_1,\omega_1) \approx \frac{2}{A^2}\left[X(2\omega_1) - \sum_{i=2}^{k} {}^x\sigma_i(2\omega_1)\right] \tag{44a}$$

$$H_2^{(x:yy)}(\omega_2,\omega_2) \approx \frac{2}{B^2}\left[X(2\omega_2) - \sum_{i=2}^{k} {}^x\sigma_i(2\omega_2)\right] \tag{44b}$$

$$H_2^{(y:xx)}(\omega_1,\omega_1) \approx \frac{2}{A^2}\left[Y(2\omega_1) - \sum_{i=2}^{k} {}^y\sigma_i(2\omega_1)\right] \tag{44c}$$

$$H_2^{(y:yy)}(\omega_2,\omega_2) \approx \frac{2}{B^2}\left[Y(2\omega_2) - \sum_{i=2}^{k} {}^y\sigma_i(2\omega_2)\right] \tag{44d}$$

$$H_2^{(x:xy)}(\omega_1,\omega_2) \approx \frac{1}{AB}\left[X(\omega_1+\omega_2) - \sum_{i=2}^{k} {}^x\sigma_i(\omega_1+\omega_2)\right] \tag{44e}$$

$$H_2^{(y:xy)}(\omega_1,\omega_2) \approx \frac{1}{AB}\left[Y(\omega_1+\omega_2) - \sum_{i=2}^{k} {}^y\sigma_i(\omega_1+\omega_2)\right]. \tag{44f}$$

In the above, second-order response harmonic amplitudes $X(2\omega_1)$, $X(2\omega_2)$, $X(\omega_1+\omega_2)$, $Y(2\omega_1)$, $Y(2\omega_2)$ and $Y(\omega_1+\omega_2)$ are filtered from the measured response. Preliminary estimates of the second-order kernel transforms are obtained after neglecting the contributions from the higher-order terms. These kernel transforms can be related to the set of six non-linear parameters, using Eq. (32), as

$$\begin{Bmatrix} H_2^{(x:xx)}(\omega_1,\omega_1) \\ H_2^{(y:xx)}(\omega_1,\omega_1) \\ H_2^{(x:yy)}(\omega_2,\omega_2) \\ H_2^{(y:yy)}(\omega_2,\omega_2) \\ H_2^{(x:xy)}(\omega_1,\omega_2) \\ H_2^{(y:xy)}(\omega_1,\omega_2) \end{Bmatrix} = \begin{bmatrix} [P^{(xx)}] & [Q^{(xx)}] \\ [P^{(yy)}] & [Q^{(yy)}] \\ [P^{(xy)}] & [Q^{(xy)}] \end{bmatrix} \begin{Bmatrix} k_{2x}^{(xx)} \\ k_{2x}^{(yy)} \\ k_{2x}^{(xy)} \\ k_{2y}^{(xx)} \\ k_{2y}^{(yy)} \\ k_{2y}^{(xy)} \end{Bmatrix} \tag{45}$$

where

$$[P^{(\eta_1\eta_2)}] = \begin{bmatrix} H_1^{(x:x)}(m\omega_1+n\omega_2) & H_1^{(x:y)}(m\omega_1+n\omega_2) \\ H_1^{(y:x)}(m\omega_1+n\omega_2) & H_1^{(y:y)}(m\omega_1+n\omega_2) \end{bmatrix} \begin{bmatrix} G_1^{(\eta_1\eta_2)} & G_2^{(\eta_1\eta_2)} & G_3^{(\eta_1\eta_2)} \\ 0 & 0 & 0 \end{bmatrix} \tag{46a}$$

and

$$[Q^{(\eta_1\eta_2)}] = \begin{bmatrix} H_1^{(x:x)}(m\omega_1+n\omega_2) & H_1^{(x:y)}(m\omega_1+n\omega_2) \\ H_1^{(y:x)}(m\omega_1+n\omega_2) & H_1^{(y:y)}(m\omega_1+n\omega_2) \end{bmatrix} \begin{bmatrix} 0 & 0 & 0 \\ G_1^{(\eta_1\eta_2)} & G_2^{(\eta_1\eta_2)} & G_3^{(\eta_1\eta_2)} \end{bmatrix} \tag{46b}$$

with notations $G_1^{(\eta_1\eta_2)}$, $G_2^{(\eta_1\eta_2)}$, $G_3^{(\eta_1\eta_2)}$ as explained in Eq. (33). The combination tone $m\omega_1 + n\omega_2$ represents the second-order harmonics selected for response amplitude measurement.

Regression of Eq. (45) with the set of measured second-order kernel transforms gives the preliminary estimates of the six non-linear parameters in the vector $\{K_2\}$. The measurements of second-order kernel transforms can also be obtained for a number of frequency sets $(\omega_1, \omega_2)_i$, and the resultant overdetermined system of equations can be solved by taking generalised inverse of the coefficient matrix formed from Eq. (45).

6.3. Preliminary estimates of third-order non-linear parameters

The third-order non-linear parameter vector, $\{K_3\}$, has in general eight unknown parameters and can be estimated through measurement of eight response harmonic amplitudes $X(3\omega_1)$, $X(3\omega_2)$, $Y(3\omega_1)$, $Y(3\omega_2)$, $X(2\omega_1+\omega_2)$, $X(2\omega_2+\omega_1)$, $Y(2\omega_1+\omega_2)$ and $Y(2\omega_2+\omega_1)$. For measurement of the corresponding third-order kernel transforms, the following k-term truncations of series expressions in Eqs. (39) and (40) are employed:

$$H_3^{(x:xxx)}(\omega_1,\omega_1,\omega_1) \approx \frac{4}{A^3}\left[X(3\omega_1) - \sum_{i=2}^{k} {}^{x}\sigma_i(3\omega_1)\right] \tag{47a}$$

$$H_3^{(x:yyy)}(\omega_2,\omega_2,\omega_2) \approx \frac{4}{B^3}\left[X(3\omega_2) - \sum_{i=2}^{k} {}^{x}\sigma_i(3\omega_2)\right] \tag{47b}$$

$$H_3^{(x:xxy)}(\omega_1,\omega_1,\omega_2) \approx \frac{4}{3A^2B}\left[X(2\omega_1+\omega_2) - \sum_{i=2}^{k} {}^{x}\sigma_i(2\omega_1+\omega_2)\right] \tag{47c}$$

$$H_3^{(x:xyy)}(\omega_1,\omega_2,\omega_2) \approx \frac{4}{3AB^2}\left[X(2\omega_2+\omega_1) - \sum_{i=2}^{k}{}^{x}\sigma_i(2\omega_2+\omega_1)\right] \tag{47d}$$

$$H_3^{(y:xxx)}(\omega_1,\omega_1,\omega_1) \approx \frac{4}{A^3}\left[Y(3\omega_1) - \sum_{i=2}^{k}{}^{y}\sigma_i(3\omega_1)\right] \tag{47e}$$

$$H_3^{(y:yyy)}(\omega_2,\omega_2,\omega_2) \approx \frac{4}{B^3}\left[Y(3\omega_2) - \sum_{i=2}^{k}{}^{y}\sigma_i(3\omega_2)\right] \tag{47f}$$

$$H_3^{(y:xxy)}(\omega_1,\omega_1,\omega_2) \approx \frac{4}{3A^2B}\left[Y(2\omega_1+\omega_2) - \sum_{i=2}^{k}{}^{y}\sigma_i(2\omega_1+\omega_2)\right] \tag{47g}$$

$$H_3^{(y:xyy)}(\omega_1,\omega_2,\omega_2) \approx \frac{4}{3AB^2}\left[Y(2\omega_2+\omega_1) - \sum_{i=2}^{k}{}^{y}\sigma_i(2\omega_2+\omega_1)\right]. \tag{47h}$$

Third-order response harmonic amplitudes $X(3\omega_1)$, $X(3\omega_2)$, $Y(3\omega_1)$, $Y(3\omega_2)$, $X(2\omega_1+\omega_2)$, $X(2\omega_2+\omega_1), Y(2\omega_1+\omega_2)$ and $Y(2\omega_2+\omega_1)$ are filtered from the measured response. Neglecting contributions from the higher-order terms, preliminary estimates of the third-order kernel transforms are obtained. These kernel transforms can be related to the set of eight non-linear parameters, using Eq. (38), as

$$\begin{Bmatrix} H_3^{(x:xxx)}(\omega_1,\omega_1,\omega_1) \\ H_3^{(y:xxx)}(\omega_1,\omega_1,\omega_1) \\ H_3^{(x:yyy)}(\omega_2,\omega_2,\omega_2) \\ H_3^{(y:yyy)}(\omega_2,\omega_2,\omega_2) \\ H_3^{(x:xxy)}(\omega_1,\omega_1,\omega_2) \\ H_3^{(y:xxy)}(\omega_1,\omega_1,\omega_2) \\ H_3^{(x:xyy)}(\omega_1,\omega_2,\omega_2) \\ H_3^{(y:xyy)}(\omega_1,\omega_2,\omega_2) \end{Bmatrix} - \begin{bmatrix} [P^{(xxx)}] & [Q^{(xxx)}] \\ [P^{(yyy)}] & [Q^{(yyy)}] \\ [P^{(xxy)}] & [Q^{(xxy)}] \\ [P^{(xyy)}] & [Q^{(xyy)}] \end{bmatrix} \begin{Bmatrix} k_{2x}^{(xx)} \\ k_{2x}^{(yy)} \\ k_{2x}^{(xy)} \\ k_{2y}^{(xx)} \\ k_{2y}^{(yy)} \\ k_{2y}^{(xy)} \end{Bmatrix} = \begin{bmatrix} [U^{(xxx)}] & [V^{(xxx)}] \\ [U^{(yyy)}] & [V^{(yyy)}] \\ [U^{(xxy)}] & [V^{(xxy)}] \\ [U^{(xyy)}] & [V^{(xyy)}] \end{bmatrix} \begin{Bmatrix} k_{3x}^{(xxx)} \\ k_{3x}^{(yyy)} \\ k_{3x}^{(xxy)} \\ k_{3x}^{(xyy)} \\ k_{3y}^{(xxx)} \\ k_{3y}^{(yyy)} \\ k_{3y}^{(xxy)} \\ k_{3y}^{(xyy)} \end{Bmatrix} \tag{48}$$

where

$$[P^{(\eta_1\eta_2\eta_3)}] = \begin{bmatrix} H_1^{(x:x)}(m\omega_1+n\omega_2) & H_1^{(x:y)}(m\omega_1+n\omega_2) \\ H_1^{(y:x)}(m\omega_1+n\omega_2) & H_1^{(y:y)}(m\omega_1+n\omega_2) \end{bmatrix} \begin{bmatrix} T_1^{(\eta_1\eta_2\eta_3)} & T_2^{(\eta_1\eta_2\eta_3)} & T_3^{(\eta_1\eta_2\eta_3)} \\ 0 & 0 & 0 \end{bmatrix} \tag{49a}$$

$$[Q^{(\eta_1\eta_2\eta_3)}] = \begin{bmatrix} H_1^{(x:x)}(m\omega_1+n\omega_2) & H_1^{(x:y)}(m\omega_1+n\omega_2) \\ H_1^{(y:x)}(m\omega_1+n\omega_2) & H_1^{(y:y)}(m\omega_1+n\omega_2) \end{bmatrix} \begin{bmatrix} 0 & 0 & 0 \\ T_1^{(\eta_1\eta_2\eta_3)} & T_2^{(\eta_1\eta_2\eta_3)} & T_3^{(\eta_1\eta_2\eta_3)} \end{bmatrix} \tag{49b}$$

and

$$[U^{(\eta_1\eta_2\eta_3)}] = \begin{bmatrix} H_1^{(x:x)}(m\omega_1 + n\omega_2) & H_1^{(x:y)}(m\omega_1 + n\omega_2) \\ H_1^{(y:x)}(m\omega_1 + n\omega_2) & H_1^{(y:y)}(m\omega_1 + n\omega_2) \end{bmatrix} \begin{bmatrix} S_1^{(\eta_1\eta_2\eta_3)} & S_2^{(\eta_1\eta_2\eta_3)} & S_3^{(\eta_1\eta_2\eta_3)} & S_4^{(\eta_1\eta_2\eta_3)} \\ 0 & 0 & 0 & 0 \end{bmatrix} \quad (49c)$$

$$[V^{(\eta_1\eta_2\eta_3)}] = \begin{bmatrix} H_1^{(x:x)}(m\omega_1 + n\omega_2) & H_1^{(x:y)}(m\omega_1 + n\omega_2) \\ H_1^{(y:x)}(m\omega_1 + n\omega_2) & H_1^{(y:y)}(m\omega_1 + n\omega_2) \end{bmatrix} \begin{bmatrix} 0 & 0 & 0 & 0 \\ S_1^{(\eta_1\eta_2\eta_3)} & S_2^{(\eta_1\eta_2\eta_3)} & S_3^{(\eta_1\eta_2\eta_3)} & S_4^{(\eta_1\eta_2\eta_3)} \end{bmatrix}. \quad (49d)$$

Notations $T_i^{(\eta_1\eta_2\eta_3)}$ and $S_i^{(\eta_1\eta_2\eta_3)}$ are as explained in Eqs. (36) and (37). The combination tone $m\omega_1 + n\omega_2$ represents the eight third-order harmonics selected for response amplitude measurement.

Regression of Eq. (48) with the set of measured third-order kernel transforms gives the preliminary estimates of the eight non-linear parameters in the vector $\{K_3\}$. The measurements of third-order kernel transforms can be obtained for a number of frequency sets $(\omega_1, \omega_2)_i$, and the resultant overdetermined system of equations can be solved as discussed before.

6.4. Iterative refinement

The preliminary estimates of the non-linear parameter vectors $\{K_2\}$ and $\{K_3\}$ are now employed to compute the previously ignored higher-order terms, ${}^x\sigma_i(m_1\omega_1 + m_2\omega_2)$, ${}^y\sigma_i(m_1\omega_1 + m_2\omega_2)$, in Eqs. (43), (44) and (47), to get refined estimates of first-, second- and third-order kernel transforms, respectively. The fresh estimates of the kernel transforms are used to regress the values of the second- and third-order non-linear parameters from Eqs. (45) and (48), respectively. The iterative process is continued to obtain converged values of these parameters. The number k of the higher-order terms to be included in the refinement would be dependent on the convergence limit for the applied excitation amplitudes and frequencies. The convergence limit can be applied through ratio test, while computing the successive higher-order terms. For accurate and convergent parameter estimation, the following issues need to be addressed:

(i) selection of appropriate excitation levels, A_i and B_i, for error minimisation in the first response harmonic measurement;
(ii) selection of limiting number of terms, k, in the finite series approximation;
(iii) selection of appropriate excitation frequency and amplitude for good measurability of higher response harmonics.

7. Convergence and error

Consider a simplified two-degree-of-freedom model with cubic non-linearity alone. The equations of motion 24(a) and 24(b) then reduce to

$$m_x\ddot{x}(t) + c_{xx}\dot{x}(t) + k_{xx}x(t) + k_{xy}y(t) + k_{3x}^{(xxx)}x^3(t) + k_{3x}^{(yyy)}y^3(t) = f_x(t) \quad (50a)$$

$$m_y\ddot{y}(t) + c_{yy}\dot{y}(t) + k_{yx}x(t) + k_{yy}y(t) + k_{3y}^{(xxx)}x^3(t) + k_{3y}^{(yyy)}y^3(t) = f_y(t). \quad (50b)$$

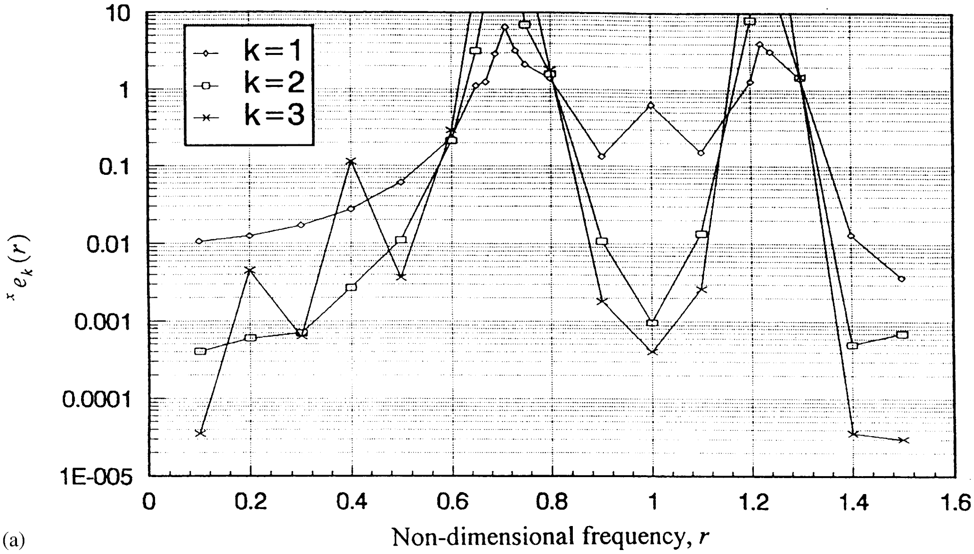

(a)

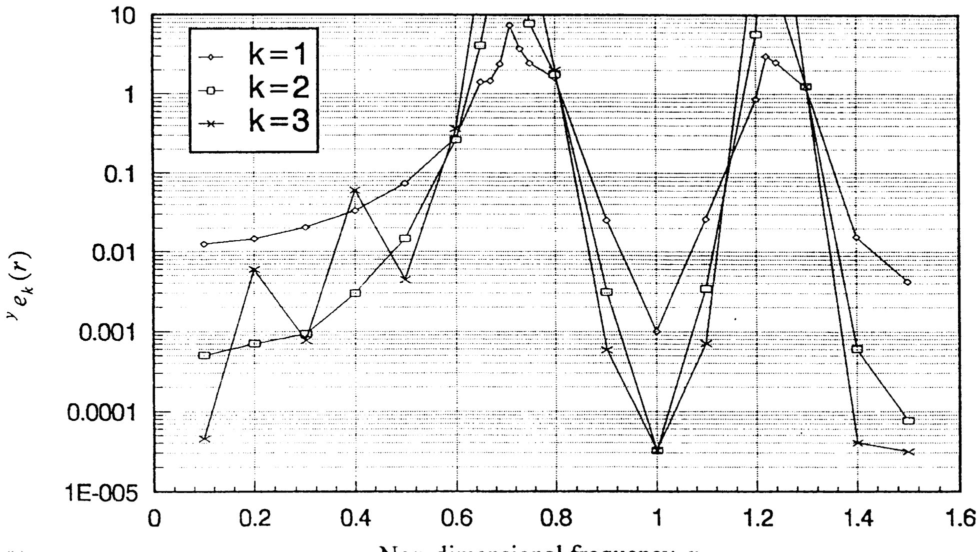

(b)

Fig. 1. Variation of series approximation error in response harmonics $X(\omega)$ and $Y(\omega)[\lambda_{xy}^N = \lambda_{yx}^N = 0.005]$: (a) error in $X(\omega)$ and (b) error in $Y(\omega)$.

Such a system can typically represent a rigid rotor supported in flexible bearings [15]. Here, k_{xx}, k_{yy} are the direct linear stiffness coefficients and k_{xy}, k_{yx} are the linear cross-coupling stiffness coefficients. $k_{3x}^{(xxx)}, k_{3y}^{(yyy)}$ are the direct non-linear stiffness coefficients, while $k_{3y}^{(xxx)}, k_{3x}^{(yyy)}$ represent the non-linear cross-coupling terms. A detailed convergence analysis has been carried out by the

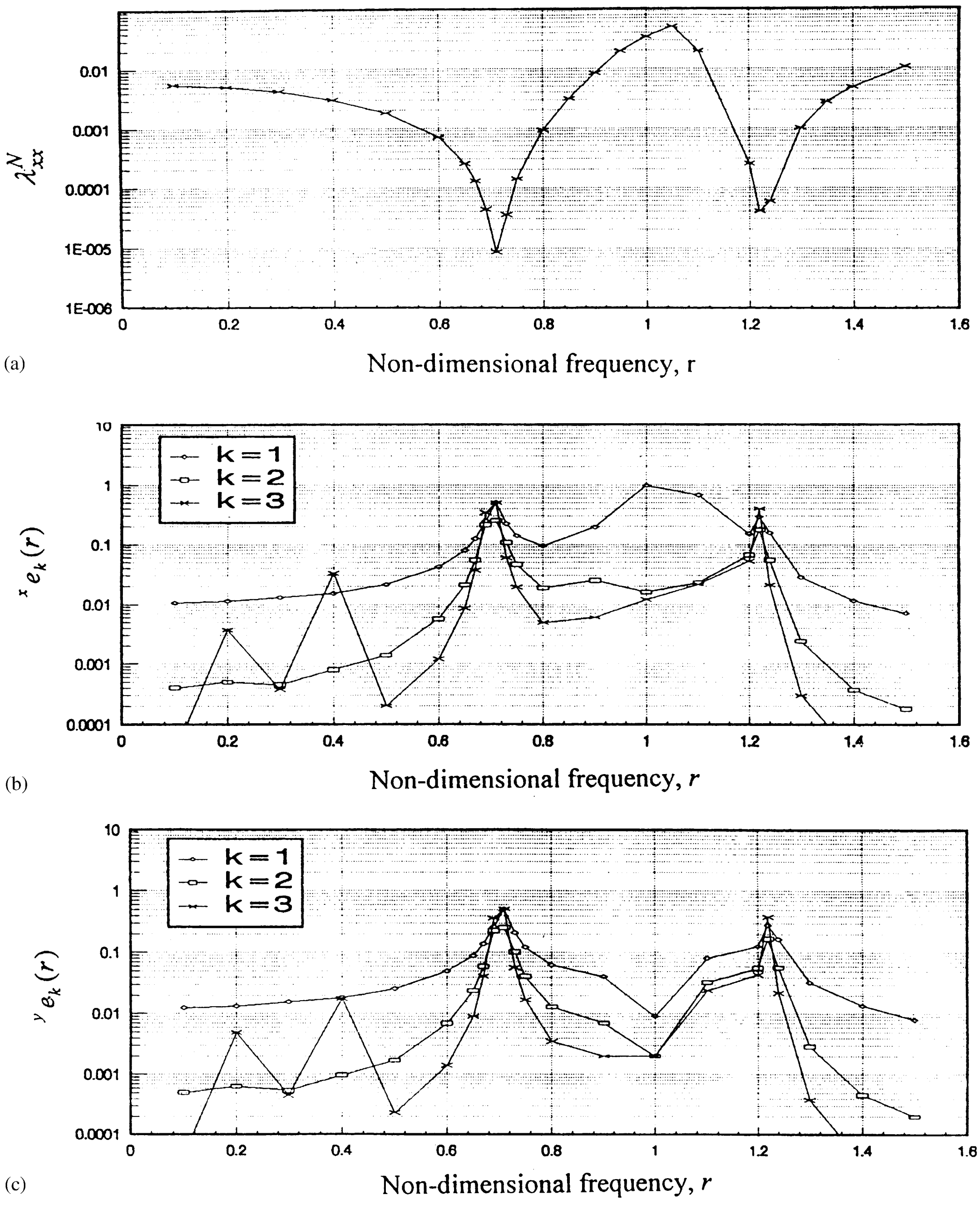

Fig. 2. Variation in series approximation error with excitation level selected for constant response harmonic amplitude: (a) variation in excitation level; (b) error in $X(\omega)$; and (c) error in $Y(\omega)$.

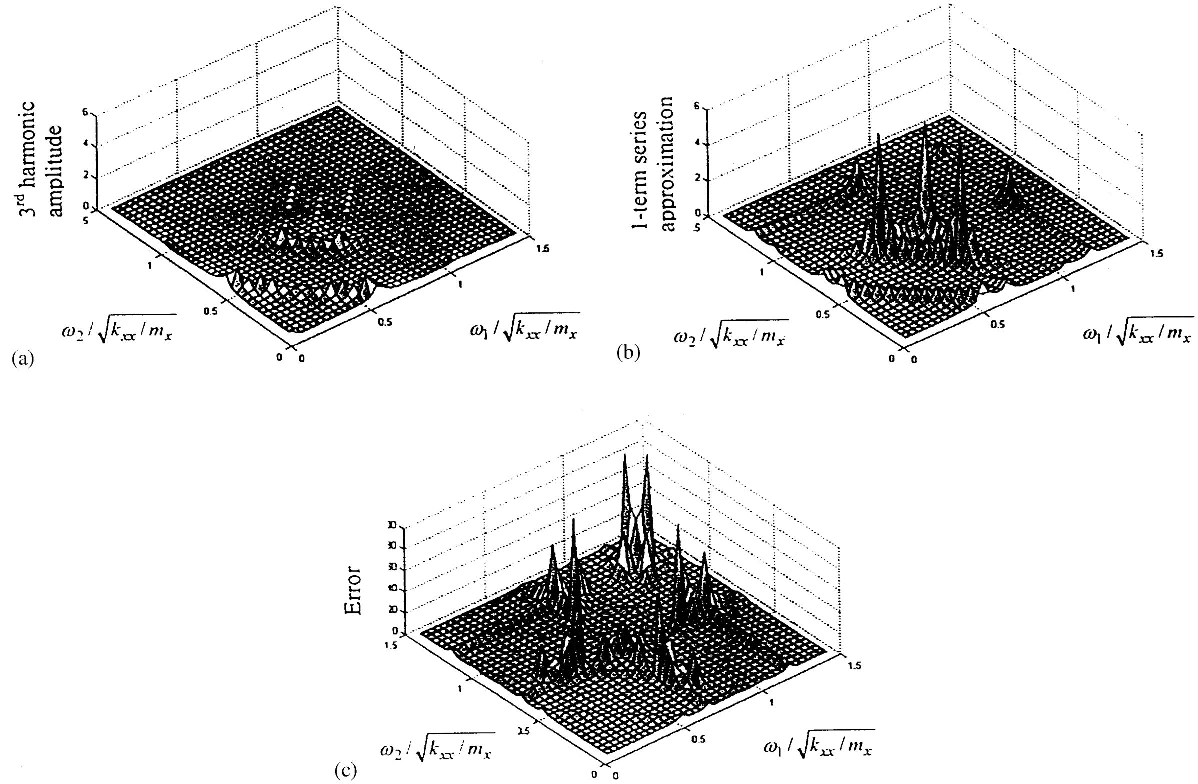

Fig. 3. Third-harmonic amplitude, $X(\omega_1+\omega_2+\omega_3)$, and the error in single-term series approximation $[\omega_3 = 0.1\times\sqrt{k_{xx/m_x}}]$: (a) third harmonic $X(\omega_1+\omega_2+\omega_3)$; (b) single-term series approximation; and (c) error of approximation.

authors in an earlier work [10] in terms of the non-dimensional parameters defined as

$$\tau=\sqrt{k_{xx}/m_x}t,\quad {}^{x}\eta(\tau)=x/X_{st},\quad {}^{y}\eta(\tau)=y/X_{st},\quad X_{st}=f_{\max}/k_{xx}\bar{f}_i(\tau)=f_i(\tau)/f_{\max},\quad i=x,y$$

$$\varsigma_{ii}=\frac{c_{ii}}{2\sqrt{k_{xx}m_x}},\quad \lambda_{ij}^{L}=\frac{k_{ij}}{k_{xx}},\quad i=x,y \text{ and } j=x,y,\quad \mu=m_y/m_x$$

$$\lambda_{xx}^{N}=\frac{k_{3x}^{(xxx)}f_{\max}^{2}}{k_{xx}^{3}},\quad \lambda_{yy}^{N}=\frac{k_{3y}^{(yyy)}f_{\max}^{2}}{k_{xx}^{3}},\quad \lambda_{xy}^{N}=\frac{k_{3x}^{(yyy)}f_{\max}^{2}}{k_{xx}^{3}},\quad \lambda_{yx}^{N}=\frac{k_{3y}^{(xxx)}f_{\max}^{2}}{k_{xx}^{3}}.$$

The error of finite term response series approximation is defined as

$${}^{\kappa}e_k(nr)=\|[{}^{\kappa}Z(nr)-{}^{\kappa}_{k}Z(nr)]/{}^{\kappa}Z(nr)|$$

where ${}^{\kappa}Z(nr)$ is the nth-order response harmonic amplitude in non-dimensional form and can be represented as

$${}^{\kappa}Z(nr)=2\sum_{i=1}^{\infty}\left(\frac{1}{2}\right)^{n}{}^{n+2i-2}C_{i-1}{}^{\kappa}H_{n+2i-2}^{n+i-1,i-1}(r),\quad \kappa=x \text{ or } y \tag{51}$$

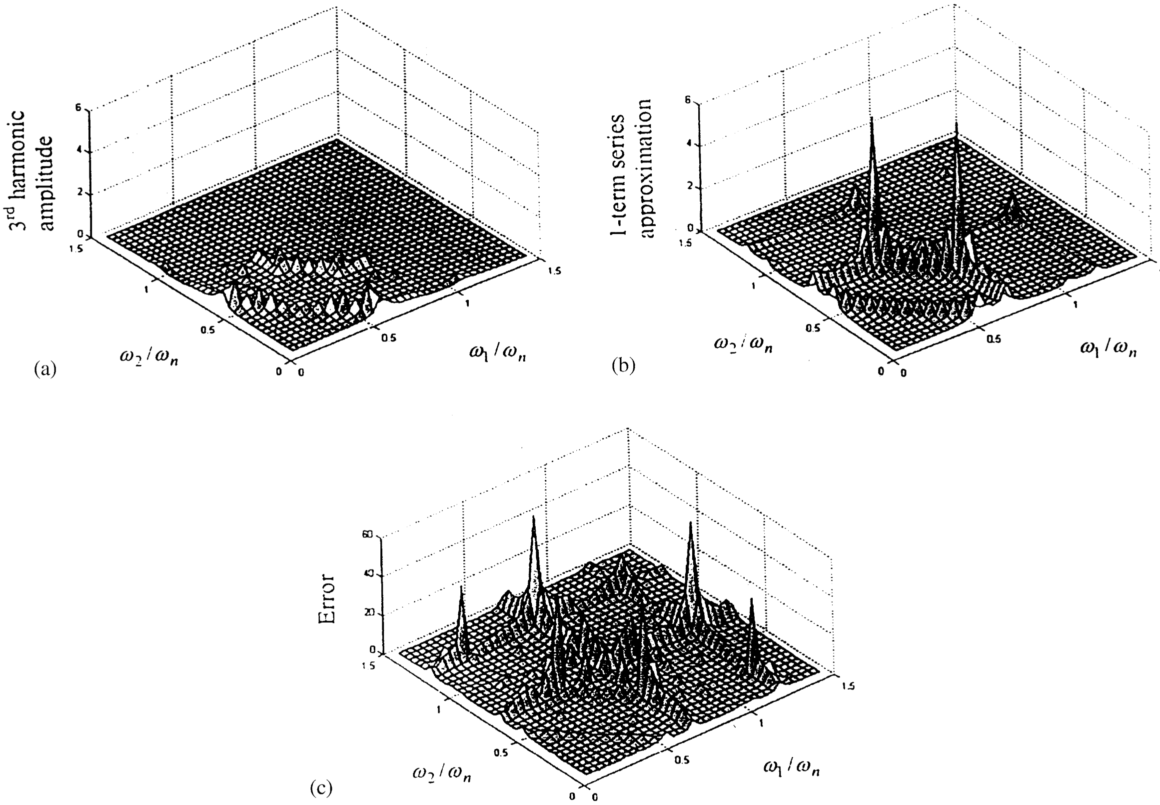

Fig. 4. Third-harmonic amplitude, $Y(\omega_1+\omega_2+\omega_3)$, and the error in single-term series approximation [$\omega_3 = 0.1 \times \sqrt{k_{xx/m_z}}$]: (a) third harmonic amplitude; (b) single-term series approximation; and (c) error of approximation.

and ${}^{\kappa}_{k}Z(nr)$ is the k-term approximation of the response series given by

$$ {}^{\kappa}_{k}Z(nr) = \sum_{i=1}^{k} {}^{\kappa}\sigma_i(nr) \tag{52}$$

where

$$ {}^{\kappa}\sigma_i(nr) = 2\left(\frac{1}{2}\right)^{n}\, {}^{n+2i-2}C_{i-1}\, {}^{\kappa}H^{(n+i-1,i-1)}_{n+2i-2}(r). \tag{53}$$

A numerical simulation on convergence and error characteristics has been carried out with

$$\mu = 1.0, \quad \lambda^{L}_{xx} = \lambda^{L}_{yy} = 1.0, \quad \lambda^{L}_{xy} = \lambda^{L}_{yx} = 0.5, \quad \varsigma_{xx} = \varsigma_{yy} = 0.01.$$

Figs. 1(a) and (b) show the variation of approximation errors ${}^{x}e_k(r)$ and ${}^{y}e_k(r)$ under constant excitation amplitudes for various number of series terms over the frequency range. It can be seen from these figures that approximation errors are very high near the natural frequencies ($r = \omega/\sqrt{k_{xx}/m_x} = 0.71$ and 1.224) and at their subharmonics. It has also been observed [10] that the critical values of the non-dimensional non-linear parameters ${}^{n}_{k}\lambda^{(\kappa)}_{\text{crit}}$ for $\kappa = x$ or y are small at the system natural frequencies and their subharmonics. The excitation

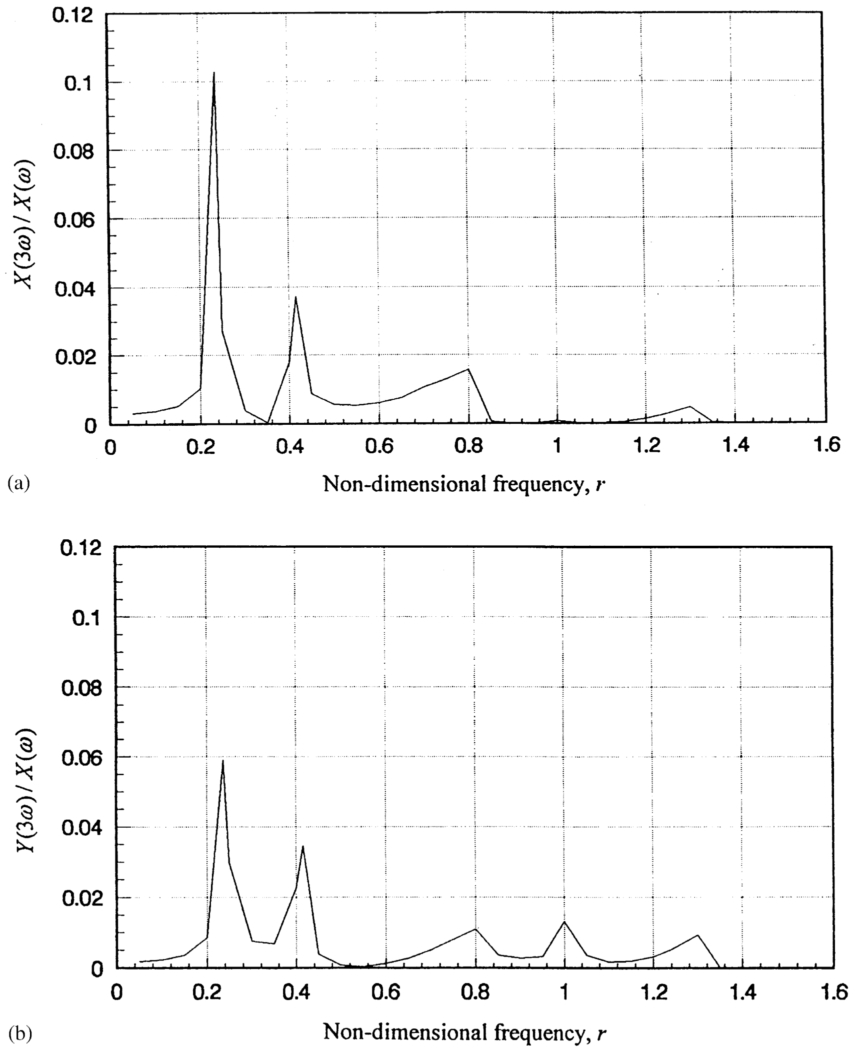

Fig. 5. Measurability of third response harmonics over the frequency range, with excitation level corresponding to $\lambda_{xx}^N = \lambda_{yy}^N = 0.005$: (a) response harmonic $X(\omega)$ and (b) response harmonic $Y(3\omega)$.

levels should therefore be kept low near natural frequencies of the system. It is desirable to have a uniform error throughout the frequency range of interest. However, in system identification problems, it is not possible to predetermine the excitation levels for uniform error, in the absence of a priori information about the unknown parameters. Alternately, excitation level can be selected by constant response amplitude criterion. Fig. 2(a) shows a variation in the excitation force, in terms of non-dimensional non-linear parameter, λ_{xx}^N, controlled for constant harmonic amplitude, $X(\omega)$. Approximation errors in the response harmonics, $X(\omega)$ and $Y(\omega)$, are plotted in Figs. 2(b) and (c), respectively. Errors are relatively high near the natural frequencies, but they are much less compared to constant excitation level case (Fig. 1(a)).

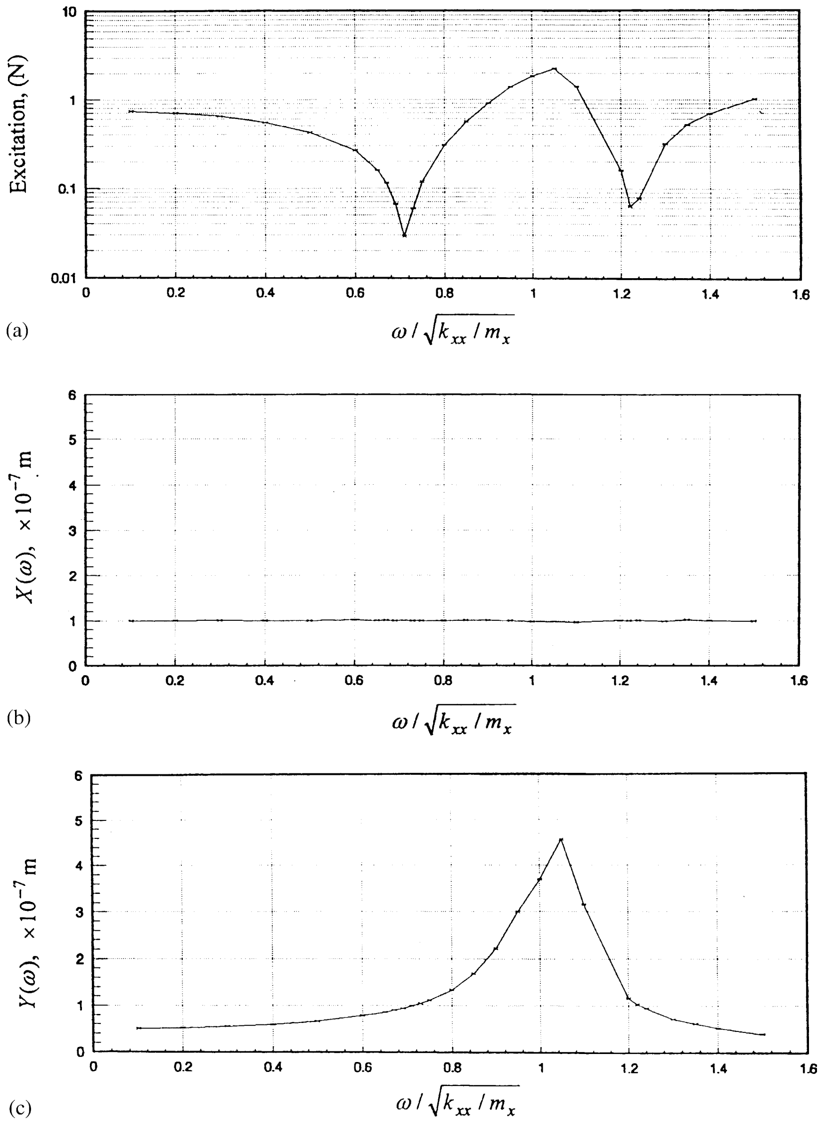

Fig. 6. Variation in excitation level for constant harmonic amplitude, $X(\omega)$, and the corresponding response harmonic amplitudes: (a) variation in excitation level; (b) harmonic amplitude, $X(\omega)$; and (c) harmonic amplitude, $Y(\omega)$.

8. Measurability of higher harmonics

Estimation of non-linear parameters is done through the measurement of higher-order harmonic amplitudes. However, these harmonic amplitudes are generally small in comparison to the fundamental harmonic amplitude for weakly non-linear systems and may be of the same order of noise or background vibration signal level. It is therefore important to design the experiment suitably to make the higher harmonics of significant amplitude so as to be distinctly measurable in

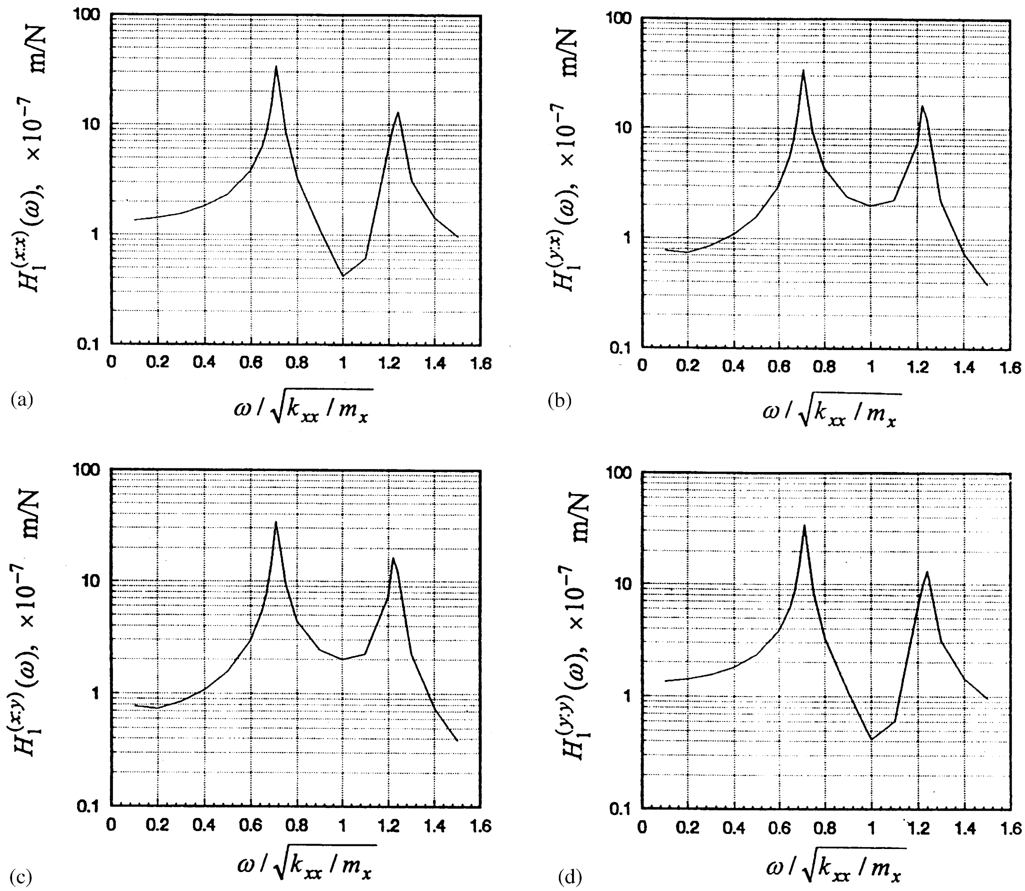

Fig. 7. Preliminary estimates of first-order kernel transforms (Case: 1): (a) kernel transform $H_1^{(x:x)}(\omega)$; (b) kernel transform $H_1^{(y:x)}(\omega)$; (c) kernel transform $H_1^{(x:y)}(\omega)$; and (d) kernel transform $H_1^{(y:y)}(\omega)$.

the response spectrum. Non-dimensional response amplitude of general third-order harmonics $X(\omega_1 + \omega_2 + \omega_3)$ and $Y(\omega_1 + \omega_2 + \omega_3)$ is plotted in Figs. 3 and 4, respectively, for ω_1 and ω_2 varying over a wide range with ω_3 being kept constant at $0.1\sqrt{k_{xx}/m_x}$. These plots have been obtained through numerical simulation using fourth-order Runge-Kutta algorithm, with three-tone excitation of the non-linear system given by Eqs. (50a) and (50b). This numerical solution can be termed as *exact* response. Figs. 3(a) and 4(a) show that the third-harmonic amplitudes are significant or measurable only along the frequency combinations $\omega_1 + \omega_2 + \omega_3 = \omega_{n_1}$ and $\omega_1 + \omega_2 + \omega_3 = \omega_{n_2}$. It may be noted here that in this case, for $\lambda_{xy}^L = \lambda_{yx}^L = 0.5$, $\omega_{n_1} = 0.71\sqrt{k_{xx}/m_x}$ and $\omega_{n_2} = 1.224\sqrt{k_{xx}/m_x}$. Figs. 3(b) and 4(b) show the Volterra series single-term approximation of the third-harmonic amplitude series for respective cases. Errors between these approximations and the *exact* solutions of Figs. 3(a) and 4(a) are plotted in Figs. 3(c) and 4(c). The error is seen to be relatively low along the frequency combination $\omega_1 + \omega_2 + \omega_3 = \omega_{n_1}$ or ω_{n_2}.

These observations indicate that the third-order response harmonics should be measured along the frequency combination line $\omega_1 + \omega_2 + \omega_3 = \omega_{n_1}$ or ω_{n_2}. For comparison of relative signal strength of higher harmonics with respect to the fundamental harmonic, a measurability index,

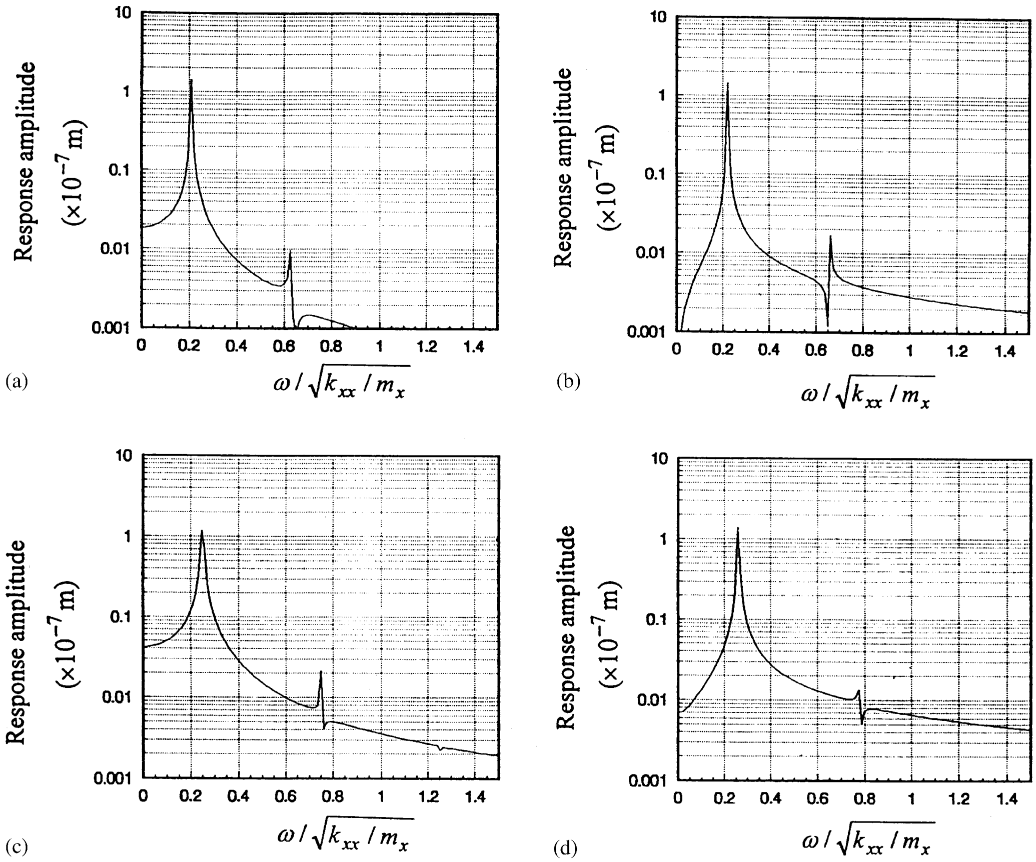

Fig. 8. Response spectrum of x-response (Case: 1, 5% measurability): (a) $\omega = 0.21\sqrt{k_{xx}/m_x}$; (b) $\omega = 0.22\sqrt{k_{xx}/m_x}$; (c) $\omega = 0.25\sqrt{k_{xx}/m_x}$; and (d) $\omega = 0.26\sqrt{k_{xx}/m_x}$.

$MI(n\omega)$, is defined as

$$MI(n\omega) = X(n\omega)/X(\omega).$$

Figs. 5(a) and (b) show the variation in measurability index over the frequency range for third harmonics $X(3\omega)$ and $Y(3\omega)$, respectively. Measurability is seen to be maximum at $\omega_{n_1}/3 = 0.237\sqrt{k_{xx}/m_x}$ and this maximum value is termed as peak measurability. These observations suggest that the third harmonic should be measured around a set of frequencies very close to one-third of first natural frequency of the system.

9. Numerical illustration

Parameter estimation is illustrated for the following values of linear and non-linear parameters in Eqs. (50a) and (50b)

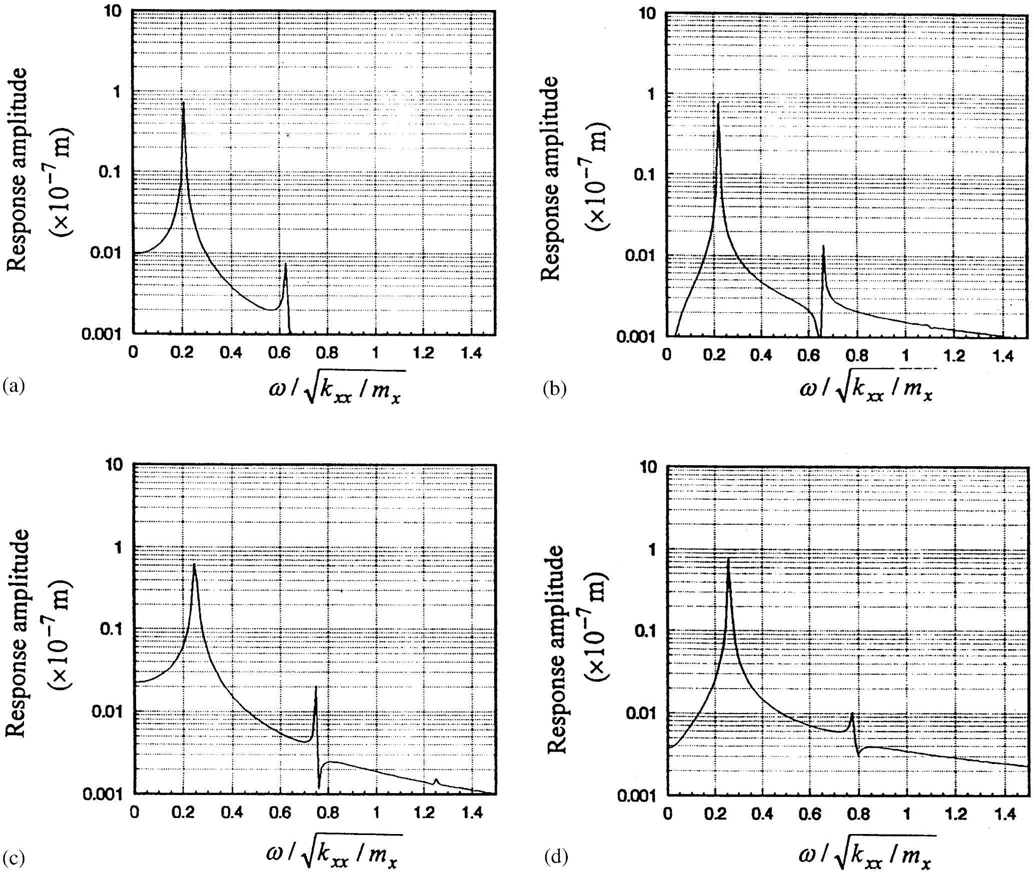

Fig. 9. Response spectrum of y-response (Case: 1, 5% measurability): (a) $\omega = 0.21\sqrt{k_{xx}/m_x}$; (b) $\omega = 0.22\sqrt{k_{xx}/m_x}$; (c) $\omega = 0.25\sqrt{k_{xx}/m_x}$; and (d) $\omega = 0.26\sqrt{k_{xx}/m_x}$.

Linear parameters:

$$m_x = m_y = 1.0\,\text{kg}$$
$$k_{xx} = k_{yy} = 1.0 \times 10^7\,\text{N/m}$$
$$\zeta_{xx} = \zeta_{yy} = 0.01$$
$$k_{xy} = k_{yx} = 0.5 \times 10^7\,\text{N/m}.$$

Non-linear parameters:

Case 1: $k_{3x}^{(xxx)} = k_{3y}^{(yyy)} = 1.0 \times 10^{19}\,\text{N/m}^3$.
Case 2: $k_{3x}^{(xxx)} = 1.0 \times 10^{19}\,\text{N/m}^3$ and $k_{3y}^{(yyy)} = 1.0 \times 10^{18}\,\text{N/m}^3$.

Response $x(t)$ and $y(t)$ are obtained from integration of equations of motion (50a) and (50b) by Runge–Kutta algorithm. For computational ease, the cross-coupled non-linear parameters $k_{3x}^{(yyy)}$ and $k_{3y}^{(xxx)}$ are taken as zero. Case 1 represents identical non-linear stiffness coefficients in both the x- and y-direction, whereas Case 2 represents asymmetrical non-linearity in x- and y-direction.

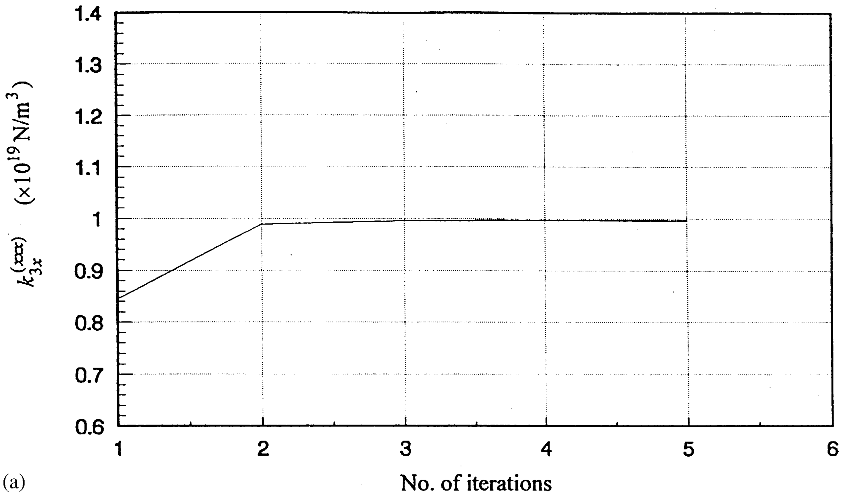

(a)

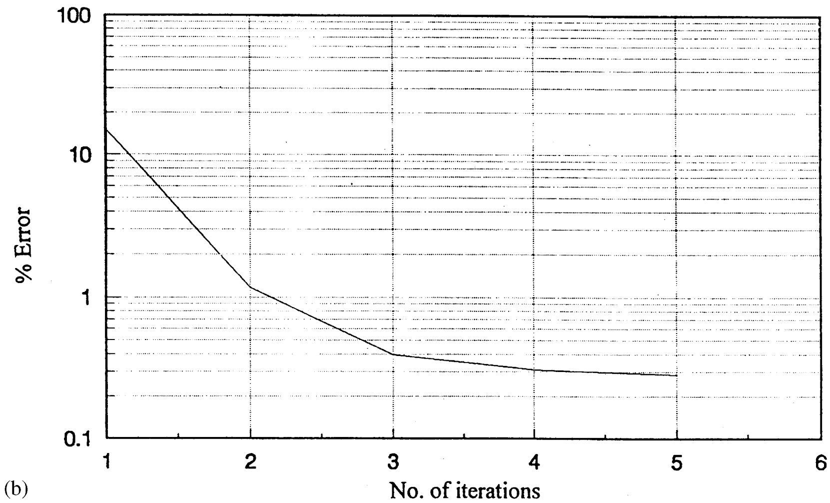

(b)

Fig. 10. (a) Iterative estimates of non-linear parameters (Case: 1, 5% measurability). (b) Convergence of estimation error with iterations (Case: 1, 5% measurability).

Single-point excitation—one at a time, first in the x-direction and then in the y-direction—is employed.

9.1. Case 1

The natural frequencies of the two-degree-freedom system under consideration are found to be $0.7\sqrt{k_{xx}/m_x}$ and $1.224\sqrt{k_{xx}/m_x}$. Frequency range, from $\omega = 0.1\sqrt{k_{xx}/m_x}$ to $\omega = 1.5\sqrt{k_{xx}/m_x}$, is selected for excitation to include both the natural frequencies. The amplitude of the harmonic excitation is varied over the frequency range so as to obtain a nearly constant response amplitude, throughout the frequency range (a constant amplitude, $X(\omega) = 1.0 \times 10^{-7}$ m, is selected in the present case). The required variation in excitation amplitude is plotted in Fig. 6(a), while the

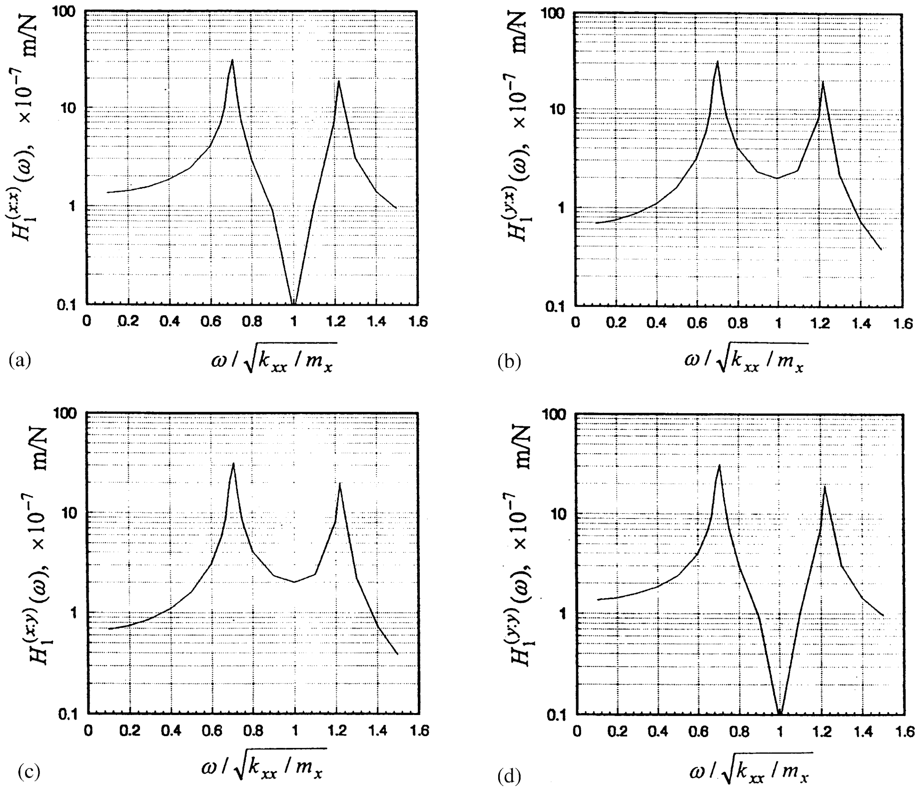

Fig. 11. Final estimates of first-order kernel transforms (Case: 1, 5% measurability): (a) kernel transform $H_1^{(x:x)}(\omega)$; (b) kernel transform $H_1^{(y:x)}(\omega)$; (c) kernel transform $H_1^{(x:y)}(\omega)$; and (d) kernel transform $H_1^{(y:y)}(\omega)$.

corresponding response levels $X(\omega)$ and $Y(\omega)$ are plotted in Figs. 6(b) and (c). The preliminary estimates of the first-order kernel transforms are obtained using Eq. (43). Excitation force is first applied in the x-direction and kernel transforms $H_1^{(x:x)}(\omega)$ and $H_1^{(y:x)}(\omega)$ are estimated. Excitation force is then applied in the y-direction, and kernel transforms $H_1^{(x:y)}(\omega)$ and $H_1^{(y:y)}(\omega)$ are estimated. Figs. 7(a)–(d) show the estimated first-order kernel transforms $H_1^{(x:x)}(\omega)$, $H_1^{(y:x)}(\omega)$, $H_1^{(x:y)}(\omega)$, and $H_1^{(y:y)}(\omega)$. Standard curve-fitting procedure is applied to these kernels to obtain the following preliminary estimates of the linear parameters:

$$k_{xx} = k_{yy} = 1.0042 \times 10^7 \text{ N/m}, \quad k_{xy} = k_{yx} = 0.4960 \times 10^7 \text{ N/m}$$
$$m_x = m_y = 0.9549 \text{ kg}, \quad \zeta_{xx} = \zeta_{yy} = 0.00883.$$

For measurement of the third-order harmonics, excitation level is set at 0.4582 N corresponding to 5% peak measurability, and response harmonic amplitudes $X(3\omega)$ and $Y(3\omega)$ are measured from the responses for a set of four excitation frequencies $\omega/\sqrt{k_{xx}/m_x} = 0.21$, 0.22, 0.25 and 0.26. These excitation frequencies are selected close to the one-third natural frequency value, $\omega_{n_1}/3 = 0.237\sqrt{k_{xx}/m_x}$. The response spectra of overall responses $x(t)$ and $y(t)$ for these excitation frequencies are shown in Figs. 8 and 9, respectively. Employing Eq. (47) and using the third-order

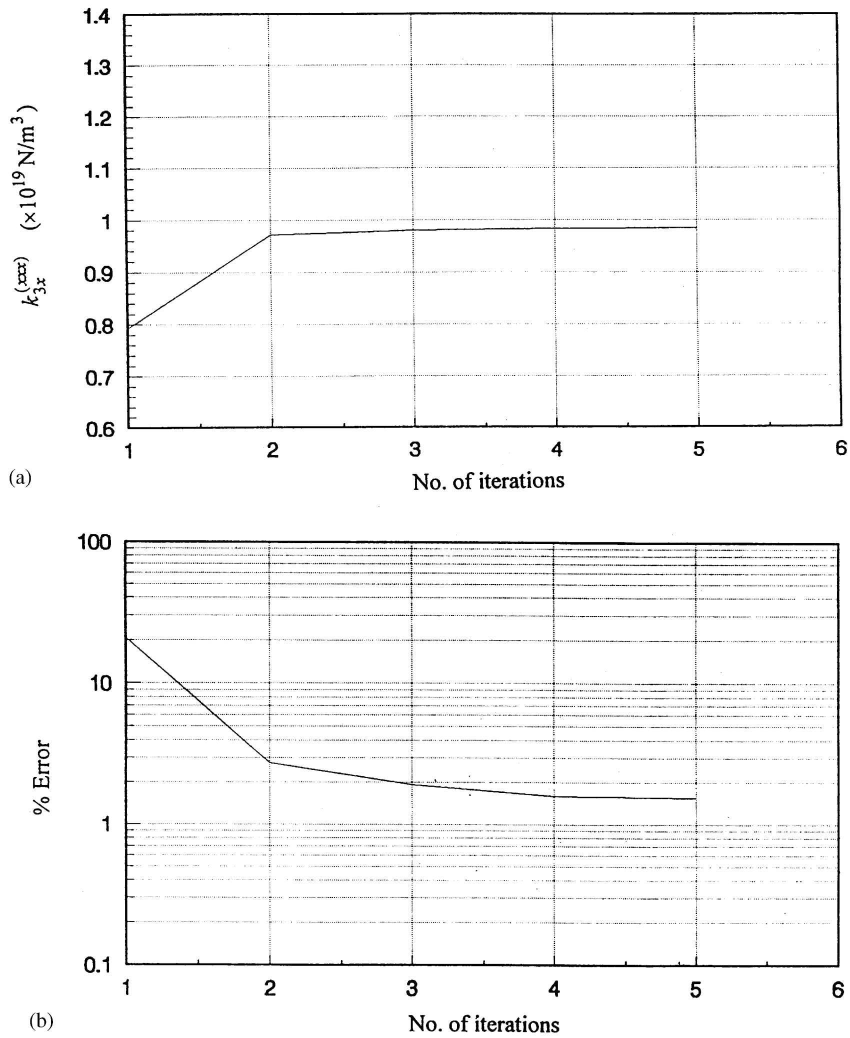

Fig. 12. (a) Iterative estimates of non-linear parameters (Case: 1, 5% measurability). (b) Convergence of estimation error with iterations (Case: 1, 5% measurability).

harmonic amplitudes, preliminary estimates of the non-linear parameters is obtained as

$$k_{3x}^{(xxx)} = k_{3y}^{(yyy)} = 0.8450 \times 10^{19}\ \mathrm{N/m^3}.$$

The recursive iteration algorithm, for refinement of the estimates, includes appropriate number of higher-order series terms in Eqs. (43) and (47) to give a convergent Volterra series solution. Iterations are continued till the estimated non-linear parameters converge within a variation range of 0.1%. Fig. 10(a) shows the convergence of iterative estimates of the non-linear parameter $k_{3x}^{(xxx)}$ with successive iterations (it is the same for the other non-linear parameter $k_{3y}^{(yyy)}$). Corresponding error of estimation is plotted in Fig. 10(b). A significant improvement in estimates is obtained

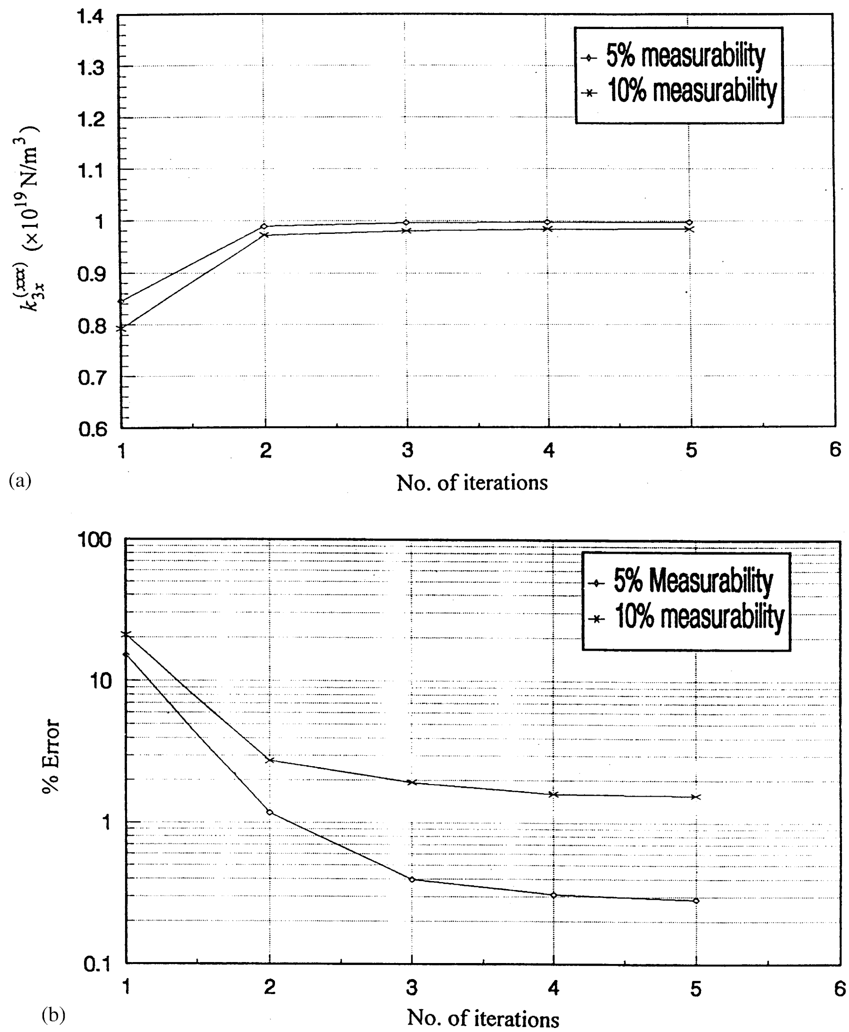

Fig. 13. (a) Comparison in estimation of non-linear parameters, between 5% measurability and 10% measurability cases (Case: 1). (b) Comparison of estimation error between 5% measurability and 10% measurability cases (Case: 1).

through iteration giving error reduction from 15% to 0.29%. Fig. 11 shows the final estimates of the first-order kernel transforms. The final estimates of linear and non-linear parameters are:

$$k_{xx} = k_{yy} = 0.9998 \times 10^7\ \text{N/m}, \quad k_{xy} = k_{yx} = 0.5088 \times 10^7\ \text{N/m}$$
$$m_x = m_y = 0.9994\ \text{kg}, \quad \zeta_{xx} = \zeta_{yy} = 0.01005$$
$$k_{3x}^{(xxx)} = k_{3y}^{(yyy)} = 0.9971 \times 10^{19}\ \text{N/m}^3.$$

A significant feature of the recursive iteration procedure is the major improvement obtained in the damping estimates. The preliminary estimate was $\zeta_{xx} = \zeta_{yy} = 0.00883$, with an error of 11.7%. The final estimate is $\zeta_{xx} = \zeta_{yy} = 0.01005$, where the error has reduced to 0.05%. This

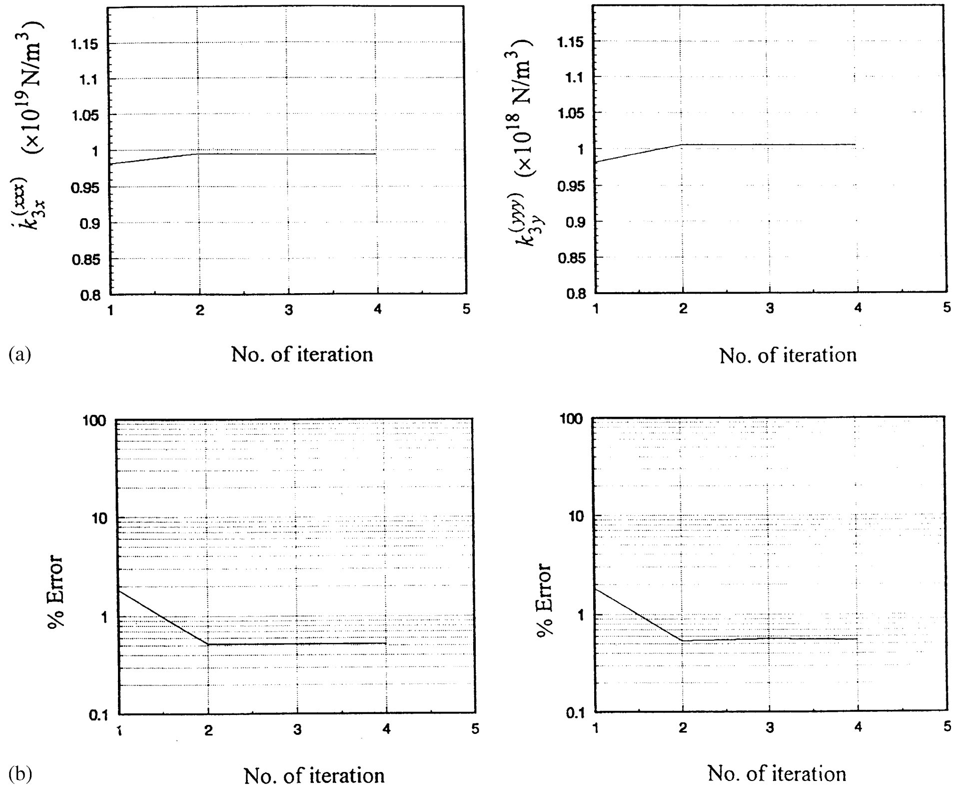

(a)

(b)

Fig. 14. (a) Iterative estimates of non-linear parameters (Case: 2, 10% measurability). (b) Convergence of estimation error with iterations (Case: 2, 10% measurability).

improvement can be explained by noting that the first-order FRF values are very much sensitive to damping near the natural frequencies and hence the accuracy of damping estimate is directly related to that of FRF estimates near natural frequencies. The procedure of excitation level control, suggested in Section 7, plays a significant role here as it employs lower excitation level near the natural frequencies, which improves convergence of the response series and enables correction with more number of higher-order terms in recursive iteration.

Similar exercise is carried out for 10% peak measurability, which is obtained at an excitation amplitude of 0.693 N. The convergence pattern for the estimates of non-linear parameters and the corresponding error are shown in Figs. 12(a) and (b). Final estimates of linear and non-linear parameters are:

$$k_{xx} = k_{yy} = 1.0010 \times 10^7\ \text{N/m}, \quad k_{xy} = k_{yx} = 0.5089 \times 10^7\ \text{N/m}$$
$$m_x = m_y = 0.9996\ \text{kg}, \quad \zeta_{xx} = \zeta_{yy} = 0.01002, \quad k_{3x}^{(xxx)} = k_{3y}^{(yyy)} = 0.9858 \times 10^{19}\ \text{N/m}^3.$$

A comparison of the above results with those obtained for the earlier case of 5% measurability reveals no significant change in the linear estimates. However, the demand for higher measurability results in higher error in estimates of non-linear parameters (1.42% in the case of 10% measurability; 0.29% in the case of 5% measurability; Figs. 13(a) and (b).

9.2. Case 2

In this case, non-linear stiffness along the y-direction is taken 0.1 times that along the x-direction. This represents an asymmetric stiffness model. The simulation is carried out with the same set of excitation levels as in Case 1, corresponding to 10% peak measurability. The convergence pattern of non-linear parameter estimates during recursive iteration, along with the associated error, is shown in Figs. 14(a) and (b). Final estimates of linear and non-linear parameters are:

$$m_x = 0.9900\,\text{kg}, \quad m_y = 1.0254\,\text{kg}$$
$$k_{xx} = 0.9828 \times 10^7\,\text{N/m}, \quad k_{xy} = 0.4997 \times 10^7\,\text{N/m}$$
$$k_{yy} = 1.0277 \times 10^7\,\text{N/m}, \quad k_{yx} = 0.4998 \times 10^7\,\text{N/m}$$
$$\zeta_{xx} = 0.00993, \quad \zeta_{yy} = 0.009927$$
$$k_{3x}^{(xxx)} = 0.9948 \times 10^{19}\,\text{N/m}^3, \quad k_{3y}^{(yyy)} = 1.0055 \times 10^{18}\,\text{N/m}^3.$$

Final estimation errors are 0.52% and 0.58%, respectively, for the non-linear parameters. It is found that in this case faster convergence is achieved than in Case 1.

10. Conclusion

Multi-input Volterra series has been employed here for developing a parameter estimation procedure for multi-degree-of-freedom systems with polynomial form non-linearity. The procedure is based on recursive iteration and works with the convergence criteria developed by the authors in an earlier work. Inclusion of higher-order response component terms in harmonic amplitude improves the estimation accuracy significantly, which is evident from the comparison between preliminary estimates and final estimates. Appropriate control of excitation level over the frequency range facilitates accurate estimation of damping, which otherwise is found to be very difficult in previous procedures. The estimation algorithm, developed here for stiffness non-linearity, can be easily extended for damping non-linearity as well.

Acknowledgements

The authors express their thanks for the financial aid provided by the Propulsion Panel of Aeronautical Research and Development Board, Ministry of Defence, Government of India, in carrying out the study.

References

[1] E. Bedrosian, S.O. Rice, The output properties of Volterra systems (nonlinear system with memory) driven by harmonic and Gaussian input, Proceedings of the IEEE 59 (12) (1971) 1688–1707.
[2] M. Schetzen, Measurement of the kernels of a nonlinear system of finite order, International Journal of Control 1 (3) (1965) 251–263.
[3] M. Schetzen, A theory of nonlinear system identification, International Journal of Control 20 (4) (1974) 577–592.
[4] S. Boyd, Y.S. Tang, L.O. Chua, Measuring Volterra kernels, IEEE Transactions on Circuits and Systems CAS-30 (8) (1983) 571–577.
[5] L.O. Chua, Y. Liao, Measuring Volterra kernels (II), International Journal of Circuit Theory and Applications 17 (1989) 151–190.
[6] L.O. Chua, Y. Liao, Measuring Volterra kernels III: how to estimate the highest significant order, International Journal of Circuit Theory and Applications 19 (1991) 189–209.
[7] S.J. Gifford, Estimation of second and third order frequency response functions using truncated model, Mechanical Systems and Signal Processing 7 (2) (1993) 145–160.
[8] D.M. Storer, G.R. Tomlinson, Recent developments in the measurement and interpretation of higher order transfer functions from nonlinear structure, Mechanical Systems and Signal Processing 7 (2) (1993) 173–189.
[9] G.R. Tomlinson, G. Manson, G.M. Lee, A simple criterion for establishing an upper limit to the harmonic excitation level of the Duffing oscillator using the Volterra series, Journal of Sound and Vibration 190 (5) (1996) 751–762.
[10] A. Chatterjee, N.S. Vyas, Convergence analysis of Volterra series response of nonlinear systems subjected to harmonic excitation, Journal of Sound and Vibration 236 (2) (2000) 339–358.
[11] S.J. Gifford, G.R. Tomlinson, Recent advances in the application of functional series to nonlinear structures, Journal of Sound and Vibration 135 (2) (1989) 289–317.
[12] G.M. Lee, Estimation of nonlinear system parameters using higher order frequency response functions, Mechanical Systems and Signal Processing 11 (2) (1997) 219–228.
[13] A. Chatterjee, N.S. Vyas, Nonlinear parameter estimation through Volterra series using method of recursive iteration, Journal of Sound and Vibration, 2003, in press.
[14] K. Worden, G. Manson, G.R. Tomlinson, A harmonic probing algorithm for the multi-input Volterra series, Journal of Sound and Vibration 201 (1) (1997) 67–84.
[15] A.A. Khan, N.S. Vyas, Nonlinear bearing stiffness parameter estimation in flexible rotor-bearing systems using Volterra and Wiener Approach, Probabilistic Engineering Mechanics 6 (2) (2001) 137–157.